Title

Intercellular transmission of the unfolded protein response promotes survival and drug resistance in cancer cells

Journal

Science Signaling, 10(482)

ISSN

1945-0877

Authors

Rodvold, Jeffrey J
Chiu, Kevin T
Hiramatsu, Nobuhiko
et al.

Publication Date

2017-06-06

DOI

10.1126/scisignal.aah7177

Peer reviewed

HHS Public Access

Author manuscript

Sci Signal. Author manuscript; available in PMC 2018 May 21.

Published in final edited form as:

Sci Signal. ; 10(482): . doi:10.1126/scisignal.aah7177.

Intercellular transmission of the unfolded protein response promotes survival and drug resistance in cancer cells

Jeffrey J. Rodvold[1], **Kevin T. Chiu**[1], **Nobuhiko Hiramatsu**[2], **Julia K. Nussbacher**[3], **Valentina Galimberti**[1], **Navin R. Mahadevan**[1], **Karl Willert**[3], **Jonathan H. Lin**[2], and **Maurizio Zanetti**[1,*]

[1]Laboratory of Immunology, Department of Medicine and Moores Cancer Center, University of California at San Diego, La Jolla, CA 92093, USA.

[2]Department of Pathology, University of California at San Diego, La Jolla, CA 92093, USA.

[3]Department of Cellular and Molecular Medicine, University of California at San Diego, La Jolla, CA 92093, USA.

Abstract

Increased protein translation in cells and various factors in the tumor microenvironment can induce endoplasmic reticulum (ER) stress, which initiates the unfolded protein response (UPR). We have previously reported that factors released from cancer cells mounting a UPR induce a de novo UPR in bone marrow–derived myeloid cells, macrophages, and dendritic cells that facilitates protumorigenic characteristics in culture and tumor growth in vivo. We investigated whether this intercellular signaling, which we have termed transmissible ER stress (TERS), also operates between cancer cells and what its functional consequences were within the tumor. We found that TERS signaling induced a UPR in recipient human prostate cancer cells that included the cell surface expression of the chaperone GRP78. TERS also activated Wnt signaling in recipient cancer cells and enhanced resistance to nutrient starvation and common chemotherapies such as the proteasome inhibitor bortezomib and the microtubule inhibitor paclitaxel. TERS-induced activation of Wnt signaling required the UPR kinase and endonuclease IRE1. However, TERS-

*Corresponding author. mzanetti@ucsd.edu.

SUPPLEMENTARY MATERIALS

www.sciencesignaling.org/cgi/content/full/10/482/eaah7177/DC1

Fig. S1. TERS transmission and reception occur among various human cancer cell lines.
Fig. S2. Nutrient-starved TERS-primed cells have increased viability during nutrient deprivation.
Fig. S3. Bortezomib does not affect UPR transcription between vehicle- and TERS-primed cells but is less cytotoxic to TERS-primed cells.
Fig. S4. TERS-primed LNCaP cells are protected from paclitaxel cytotoxicity.
Fig. S5. TERS CM promotes abundance in β-catenin.
Fig. S6. Validation of PC3.TOP reporter system.
Fig. S7. MEF KO cells have selective sensitivity to TERS.
Fig. S8. Population fitness of TERS-primed cells.
Fig. S9. Histology analysis of TC1 vehicle- and TERS-primed tumors.

Author contributions: J.J.R. designed and performed the experiments, analyzed the data, and wrote the manuscript. K.T.C. designed and performed the experiments. N.H. created cell-tagging constructs, performed Western blot analysis, and aided in luciferase assays. J.K.N. designed the CRISPR system. V.G. performed TERT luciferase assay experiments. N.R.M. analyzed the data and provided suggestions for the experimental design. K.W. provided the TOP.GFP construct and provided guidance on Wnt signaling. J.H.L. provided the ATF6 reporter and provided constructive criticisms on ER-related studies. M.Z. helped design experiments and wrote the manuscript.

Competing interests: The authors declare that they have no competing interests.

induced enhancement of cell survival was predominantly mediated by the UPR kinase PERK and a reduction in the abundance of the transcription factor ATF4, which prevented the activation of the transcription factor CHOP and, consequently, the induction of apoptosis. When implanted in mice, TERS-primed cancer cells gave rise to faster growing tumors than did vehicle-primed cancer cells. Collectively, our data demonstrate that TERS is a mechanism of intercellular communication through which tumor cells can adapt to stressful environments.

INTRODUCTION

Endoplasmic reticulum (ER) stress in solid tumors results from a dysregulation of protein synthesis, folding, secretion, and aberrant glycosylation, which are heightened by microenvironmental stimuli such as nutrient deprivation, hypoxia, oxidative stress, and chronic viral infection (1, 2). To cope with ER stress, tumor cells initiate an evolutionarily conserved signaling process known as the unfolded protein response (UPR), which is coordinated by three ER transmembrane-bound sensors—inositol-requiring transmembrane kinase/endoribonuclease 1α (IRE1α), activating transcription factor 6 (ATF6), and protein kinase R–like ER kinase (PERK)—which are maintained inactive in unstressed cells through luminal association with the ER chaperone glucose-regulated protein 78 [GRP78; also known as binding immunoglobulin protein (BiP)] (3). Upon excessive client protein burden, GRP78 disassociates from these three sensor proteins to preferentially bind unfolded or misfolded proteins, enabling each sensor to activate downstream signaling cascades that attempt to normalize protein folding and secretion. PERK phosphorylates eukaryotic initiation factor 2α (eIF2α), resulting in selective inhibition of translation to reduce ER client protein load. IRE1α autophosphorylates, oligomerizes, and activates its endoribonuclease function that generates a spliced isoform of X-box binding protein–1 (XBP-1s), which drives the production of various ER chaperones. ATF6 translocates to the Golgi, where it is cleaved into its functional form and acts in tandem with XBP-1s to restore ER homeostasis (4). Persistent ER stress activates the transcription factor CCAAT/enhancer-binding protein homologous protein (CHOP), which can initiate apoptosis (5).

The role of the UPR in tumorigenesis and cancer progression is typically distinguished by cell-intrinsic functions, which enhance cell fitness and survival, and cell-extrinsic functions, which are mediated by soluble messenger molecules released by cancer cells undergoing a UPR that co-opt recipient cells (6–10). In support of the former, conditional homozygous knockout (KO) of *Grp78* in the prostate of mice with *Pten* inactivation protects against cancer growth (11), whereas the inactivation of PERK or expression of a dominant-negative PERK mutant in cancer cells yields smaller and less aggressive tumors in mice (12). Human tumor cells have high amounts of GRP78 (13), which confers resistance to chemotherapy (14). In addition, the translocation of GRP78 to the cell surface is proposed to serve as a signaling molecule that activates phosphoinositide 3-kinase (PI3K) (15, 16), which promotes proliferation. As to cell-extrinsic effects, we previously found that cancer cells undergoing a UPR can transmit ER stress to bone marrow–derived myeloid cells, macrophages, and dendritic cells (6–10) and impart these cells with a mixed proinflammatory/immunosuppressive phenotype (10) that is associated with defective activation of naïve $CD8^+$ T cells (8). The existence of a similar UPR-based cell-nonautonomous

communication in *Caenorhabditis elegans*, which promotes stress resistance and organismal longevity (17), suggests that this phenomenon may be evolutionarily conserved (18). We propose that it may also be leveraged by the tumor to promote its survival and outgrowth.

The induction of the UPR in cancer cells triggers the release of soluble factors that are able to transmit ER stress to recipient myeloid cells (7–9). We termed this phenomenon transmissible ER stress (TERS). Here, we investigated whether TERS is operative among cancer cells and what the consequence of this phenomenon might be in recipient cancer cells. Our findings reveal a hitherto unappreciated role for a UPR-based intercellular signaling mechanism within tumors through which tumor cells gain fitness and the capability to cope with metabolic, proteotoxic, or genotoxic stress. Additionally, because spatial heterogeneity in UPR activation within a tumor correlates with tumor growth rates (19), the phenomenon may ultimately contribute to the clonal heterogeneity and fitness of tumor cells in vivo.

RESULTS

Prostate cancer cells transmit ER stress to homologous and heterologous cancer cells

We generated conditioned medium (CM), herein called TERS-conditioned medium (TERS CM), using the human prostate cancer cell line PC3 cultured with the sarcoplasmic/endoplasmic reticulum Ca^{2+} (SERCA)–adenosine triphosphatase (ATPase) inhibitor thapsigargin (Tg), as previously described (7). Unstressed homologous PC3 cells (Fig. 1, A and B) or heterologous DU145 cells (Fig. 1C) were cultured in TERS CM or CM from vehicle-treated (control) cells (Veh CM) for 5 days. These “recipient” cells were harvested on days 1, 3, and 5 and analyzed by reverse transcription quantitative polymerase chain reaction (RT-qPCR) for the expression of three key UPR genes: *GRP78*, spliced *XBP-1* (*XBP-1s*), and *CHOP* (Fig. 1, A and C). GRP78 protein abundance was also analyzed by Western blot (Fig. 1B). TERS CM treatment engaged a global UPR in both cell lines throughout the 5-day culture period as well as promoted inflammation, as determined by gene expression for *IL-6* (Fig. 1D) in PC3-treated cells. ER stress transmission was not limited to human prostate cancer cells; the same phenomenon occurred in other human cancer cell lines, including breast and pancreatic cancer cells (fig. S1). This suggests that TERS, as a phenomenon, is not restricted to only affect recipient myeloid cells and is independent of the type of transmitting and recipient cancer cells.

The ER-resident chaperone GRP78 plays numerous roles in the tumorigenesis of various organs, including the prostate (20). GRP78 also translocates to the surface of prostate cancer cells (15, 16, 20), where it serves as a signaling molecule for cell growth by activating PI3K (15, 16). The 2-day treatment with TERS CM markedly increased cytoplasmic expression of GRP78 (Fig. 1E). By staining for the C terminus of GRP78, which is surface-exposed upon translocation to the cell membrane (21), we found that TERS CM provided a progressive translocation of surface GRP78 (sGRP78) that began on day 3 and persisted through day 5 (Fig. 1F). This suggests that TERS may be a stimulus to induce the translocation of GRP78 to the cell surface.

TERS endows recipient tumor cells with a unique UPR

We reasoned that because TERS CM induced the progressive translocation of the ER-resident chaperone GRP78 to the cell surface, a short-term exposure to TERS CM could alter ER function and dynamics. Tumor cells in vivo may be subject to UPR-based cell-nonautonomous effects in a transient and possibly iterative manner as a result of cell-intrinsic or tumor microenvironment–borne perturbations (6, 22). To mimic the stochastic way ER stress transmission among cancer cells may occur in vivo, naïve PC3 cells were treated with TERS CM or Veh CM for 2 days followed by a 2-day rest period in standard growth medium to enable the resolution of ER stress (Fig. 2A). At the end of the rest period, we noted that PC3 cells had a substantial increase in sGRP78 abundance (Fig. 2B). In light of previous reports that found that this translocation corresponds with improved cytoprotection and chemoresistance (23–25), we provisionally conclude that sGRP78 abundance in TERS CM–cultured cells was reflective of a functionally unique population potentially better able to cope with a subsequent UPR. We termed these cells “TERS-primed,” because this ER stress adaptation is reminiscent of earlier observations that cells exposed to protracted mild ER stress undergo an adaptive UPR (26).

To study the consequences of TERS priming on the response to physiological tumor microenvironmental stressors, TERS- and vehicle-primed PC3 cells were challenged by nutrient deprivation through culture in glucose- and serum protein–free medium for 48 hours. TERS-primed cells had increased protein abundance of GRP78 compared with vehicle-primed cells under both normal and nutrient-deprived conditions, despite the fact that nutrient starvation markedly increased GRP78 in vehicle-primed cells (Fig. 2C). We also found reduced transcriptional activation of UPR genes in the TERS-primed cells (fig. S2A). The differential expression of GRP78 led us to investigate whether PERK was also differentially affected between TERS- and vehicle-primed cells. Under nutrient (glucose and serum)–deprived conditions, we found a distinct decrease in the amount of phosphorylated PERK and eIF2α in TERS-primed cells relative to vehicle-primed cells (Fig. 2D). TERS-primed cells also displayed a marked reduction in the abundance of ATF4 and the downstream protein CHOP during nutrient deprivation (Fig. 2D). Notably, the PERK pathway in TERS-primed cells was also repressed under standard cell culture conditions relative to vehicle-primed cells. These findings suggested that TERS priming differentially affects PERK pathway activation, providing protection from CHOP-mediated apoptotic signaling due to diminished ATF4 activation. We quantified the viability of vehicle- or TERS-primed PC3 cells cultured in glucose/serum-depleted or glucose/serum-replete by annexin V staining and found that cell survival was greater in TERS-primed cultures than in vehicle-primed cultures (Fig. 2E). This cytoprotection against nutrient starvation similarly occurred in TERS-primed DU145 and LNCaP cells (fig. S2, B and C). These findings demonstrate that TERS signaling improves the recipient cancer cells’ ability to survive amidst nutrient starvation that is common in the tumor microenvironment.

TERS-primed cells are protected against proteasome inhibition–mediated toxicity

Bortezomib (Velcade) is a proteasome inhibitor used in the treatment of multiple myeloma (27) and is also proposed for the treatment of solid tumors, including prostate cancer (28, 29). Its mechanism of action involves the induction of unresolvable ER stress, leading to

apoptosis (30). We investigated whether TERS priming also impinges on bortezomib-mediated cytotoxicity. Whereas bortezomib evoked no significant transcriptional differences in UPR genes between vehicle- and TERS-primed PC3 cells (fig. S3A), the treatment of bortezomib increased total GRP78 levels in both vehicle- and TERS-primed PC3 cells. However, TERS-primed cells maintained increased protein abundance throughout the titration of the drug (Fig. 3A). These results confirm that bortezomib induces a UPR and that TERS-primed cells display a larger amount of GRP78 during bortezomib-induced stress. We found a similar trend in relation to surface abundance of GRP78: Bortezomib treatment increased sGRP78 in vehicle-primed cells, albeit modestly, as well as in TERS-primed cells relative to unstimulated conditions (Fig. 3B). However, bortezomib-treated TERS-primed cells displayed a marked increase in sGRP78 over bortezomib-treated vehicle-primed cells (Fig. 3B). The cytotoxicity of bortezomib is reportedly mediated through ATF4-dependent activation, whereas IRE1α signaling is dispensable for its effects (31). We therefore compared the relative PERK response between TERS- and vehicle-primed PC3 cells after bortezomib exposure. Although there appeared to be relatively comparable amounts of phosphorylated PERK and eIF2α in bortezomib-treated, TERS CM–cultured, or Veh CM–cultured cells, TERS-primed cells had substantially reduced abundance of ATF4 and CHOP protein relative to vehicle-primed cells in response to bortezomib (Fig. 3C). Because GRP78 and ATF4 can play cytoprotective roles, we probed the viability of TERS-and vehicle-primed PC3 cells in response to bortezomib. TERS-primed cells had improved survival over vehicle-primed cells across a 2-log titration of bortezomib (Fig. 3D). TERS-primed DU145 and LNCaP cells were similarly protected against bortezomib (fig. S3, B and C).

We next probed the durability of TERS-induced cytoprotection in bortezomib cytotoxicity. We reasoned that increased GRP78 abundance signaled the presence of an adaptive UPR pursuant to TERS priming, providing cells with a greater ability to cope with bortezomib cytotoxicity. Although GRP78 abundance decreased under both conditions in the 5 days after cells were rested (meaning, returned to normal medium), GRP78 was maintained at a greater abundance in TERS-primed cells than in vehicle-primed cells (Fig. 3E). This correlated with persistent cytoprotection from bortezomib (Fig. 3F).

TERS protects against non–UPR-mediated cytotoxicity

Cytoprotection from UPR-inducing noxae prompted us to investigate whether TERS-primed cells are also protected against genotoxicity. Paclitaxel, a microtubule stabilizer that is frequently used to treat patients with various types of solid tumors, including prostate cancer, did not induce transcriptional activation of the UPR in either vehicle- or TERS-primed PC3 cells, on the basis of UPR-related gene expression (Fig. 4A) or protein abundance (Fig. 4, B and C). Although this is at odds with a previous report that found that paclitaxel initiates a UPR (32), cell- and tissue-specific differences may account for the discrepancy. We then determined the effect of TERS priming on paclitaxel-mediated cytotoxicity. Forty-eight hours after treatment, the percentage of apoptotic cells in vehicle-primed PC3 cells was markedly higher than that in TERS-primed PC3 cells (Fig. 4D). Similar results were observed using LNCaP cells (fig. S4).

Paclitaxel promotes apoptosis in part by causing cell cycle arrest in the form of a mitotic block in early M phase or, for those cells progressing through aberrant mitosis, in G_1 phase (33, 34). Because TERS-mediated resistance to paclitaxel appeared to be independent of ER stress induction, we explored the possibility that TERS priming affects the cell cycle. A 5-bromo-2′-deoxyuridine (BrdU) analysis revealed that unstimulated TERS-primed cells were twice as enriched in the G_2/M phase compared with vehicle-primed cells (Fig. 4E), suggesting that the cytoprotective effect of TERS is derived from preventing progression through the M phase. Because the G_2/M-phase arrest enables DNA damage repair during the cell cycle before mitotic entry in response to genotoxic stress (35), we also explored whether TERS priming affects the DNA damage response caused by paclitaxel. Staining for γ-H2AX, a marker for double-stranded DNA breaks, was detected in response to paclitaxel in both vehicle- and TERS-primed PC3 cells, but TERS-primed cells had fewer γ-H2AX foci per cell than vehicle-primed cells (Fig. 4F). Collectively, we infer that these findings suggest that TERS protects cancer cells against DNA damage during chemotherapy-induced genotoxicity.

TERS promotes β-catenin–mediated Wnt signaling

One possible mechanism accounting for cytoprotection and an enrichment in the G_2/M phase could be the activation of Wnt signaling, given that it has been demonstrated that Wnt signaling is predominant during the G_2/M phase (36). Specifically, we thought that TERS could stabilize β-catenin, a subunit of the cadherin protein complex and an intracellular signal transducer of the Wnt pathway (37, 38). We analyzed PC3 cells cultured in TERS CM for 5 days and monitored the transcriptional activation of *CTNNB1* and its negative regulator, *AXIN2* (39). We found that TERS CM modestly increased *CTNNB1* transcription on day 1, which continued to increase on days 3 and 5. TERS CM also increased the transcription of *AXIN2* during the latter days (Fig. 5A). Because Wnt signaling is suppressed by degradation of β-catenin, we examined the abundance of β-catenin in LNCaP cells 48 hours after treatment and found that TERS CM increased its abundance (fig. S5). Because *AXIN2* activation occurred on day 3, the delayed kinetics suggested that TERS activation of the Wnt pathway is unlikely to involve a Wnt ligand. To better elucidate the kinetics of TERS-mediated Wnt signaling, we transduced PC3 cells with the T cell factor (TCF) optimal promoter (TOP) reporter system, which expresses green fluorescent protein (GFP) when TCF is transcriptionally activated by the nuclear translocation of β-catenin (40–42). We observed reporter activation in these cells within 24 hours of treatment with GSK-XV (fig. S6, A and B), a small-molecule inhibitor of glycogen synthase kinase–3 (GSK-3), which stimulates Wnt signaling (43). Progressive activation of the TOP reporter was observed throughout TERS priming (Fig. 5B). From these data thus far, we concluded that TERS activates Wnt signaling and likely does so independently of a canonical Wnt ligand (44). To elucidate whether Wnt signaling provides cytoprotection, we treated LNCaP cells with human recombinant, soluble WNT3a protein (rWNT3a) for 2 days and then challenged them with nutrient deprivation, bortezomib, or paclitaxel. Wnt signaling provided cytoprotection from nutrient deprivation but not from bortezomib or paclitaxel (fig. S6C). Surprisingly, rWNT3a provided no protection against paclitaxel but only against nutrient starvation. This direct way to drive Wnt signaling perhaps provides adaptive responses in cells, which do not entirely mimic TERS-mediated cytoprotection.

The observation that TERS initiates Wnt signaling is, to our knowledge, the first to suggest a link between the UPR and Wnt signaling. To see whether UPR signaling is necessary per se for TERS-mediated Wnt stimulation, PC3.TOP cells were cultured in TERS CM for 48 hours in the absence or presence of either an IRE1α inhibitor [4μ8C (45)] or a PERK inhibitor [GSK2656157 (46)] and probed for Wnt signaling using the TOP reporter system by flow cytometry. IRE1α inhibition prevented TOP expression, whereas PERK inhibition had no effect (Fig. 5, C and D). This finding suggested that TERS induces Wnt signaling through IRE1α activation. To determine whether ER stress is per se sufficient to drive Wnt signaling, we treated PC3. TOP cells with the canonical ER stress inducer tunicamycin with or without 4μ8C or GSK2656157 and analyzed TOP reporter expression. Tunicamycin did not induce TOP reporter expression (Fig. 5E), indicating that TERS-induced Wnt signaling may not occur through ER stress. That IRE1α activity was necessary for TERS-mediated Wnt signaling led us to hypothesize that IRE1α's role in TERS-induced Wnt induction was independent of its function in ER stress signaling. To investigate this hypothesis, we incubated PC3.TOP cells with rWNT3a and either 4μ8C or GSK2656157 (Fig. 5F). Unexpectedly, 4μ8C inhibited TOP expression, whereas GSK2656157 had apparently no substantial effect. These findings suggest that TERS-induced Wnt signaling in recipient cancer cells is not merely attributable to pharmacologically induced ER stress but is nevertheless dependent on IRE1α signaling. The precise mechanism(s) and their influence in TERS-mediated cytoprotection remain to be fully determined.

Because β-catenin can transcriptionally activate telomerase reverse transcriptase (TERT) (47) and TERT is reportedly cytoprotective independent of the catalytic activity of telomerase (48, 49), we hypothesized that the cytoprotective effects of TERS could be due to activation of TERT, potentially via β-catenin. To this end, we probed the effect of TERS on TERT. We found no change in *TERT* transcription in PC3 cells cultured in TERS CM for 48 hours (Fig. 5G). To confirm this finding, we used a luciferase reporter gene assay for the *TERT* promoter (50). In repeat experiments, transiently transfected LNCaP cells cultured in TERS CM for 48 hours showed no evidence of *TERT* promoter activation (Fig. 5H). However, under parallel treatment conditions, cells transfected with a luciferase reporter gene for the *ATF6* promoter had robust activation (Fig. 5H), ruling out confounding effects associated with transfection or with the potency of TERS CM. In light of these results, we then explored the possibility that the transmission of ER stress could cause the redistribution of TERT inside the cells. Previous studies showed that during oxidative stress (51) or after treatment with Tg (49), TERT gradually accumulates in the cytoplasm where it allegedly plays cytoprotective roles. By confocal microscopy, TERS CM–cultured PC3 cells showed a marked accumulation of the TERT protein in the cytoplasm compared with Veh CM–cultured cells (Fig. 5I). Collectively, these findings show a correlation between TERS and cytoplasmic TERT accumulation, which could not be established as a causal relationship between β-catenin and TERT relocalization to the cytosol. We could not also establish whether the β-catenin/Wnt/TERT axis is the sole mechanism responsible for cytoprotection. Further exploration will be needed to address this issue.

The PERK pathway mediates TERS-induced cytoprotective effects

Next, we sought to better understand the mechanism behind TERS-mediated cytoprotection, which could not be fully explained through the Wnt axis. In our initial experiments, we had noted that the PERK pathway was differentially affected in TERS-primed cells relative to control cells by there being a marked decrease in ATF4 and CHOP protein, particularly during nutrient starvation and under bortezomib stress conditions. These findings may each explain cytoprotection by TERS, independent of Wnt signaling. Concordantly, the PERK pathway and its downstream effector ATF4 have been implicated in prosurvival signaling during nutrient deprivation (52, 53) and bortezomib (31) and paclitaxel (54) cytotoxicities. We therefore hypothesized that the PERK pathway is central to the facilitation of TERS-induced cytoprotection. We leveraged mouse embryonic fibroblasts (MEFs) to first confirm that the TERS-induced cytoprotective effects existed in nontransformed cells. Wild-type MEF cells were primed with Veh CM or TERS CM generated from murine prostate cancer TRAMP C1 (TC1) cells and then challenged for 48 hours by either nutrient starvation, bortezomib, or taxol, and cell viability was determined by 7-aminoactinomycin D (7AAD) exclusion. TERS-primed MEF cells survived better than their vehicle-primed counterpart in each stress condition (Fig. 6A), confirming that TERS is not restricted to cancer cells. We next challenged *PERK* KO MEFs using the same approach and found that the cytoprotection gains in wild-type cells were lost in each instance (Fig. 6B). Furthermore, *PERK* KO MEFs had markedly reduced survival relative to control cells after a 2-day culture in TERS CM (fig. S7A). This demonstrates that the PERK pathway is key to the cellular adaptation induced by TERS, which leads to improved cell survival. On the other hand, we found that the role of IRE1α and ATF6 was not as unambiguous, in that *IRE1*α and *ATF6* KO MEFs did not have complete loss of cytoprotection across the three challenge conditions as it was in the case of *PERK* KO cells (fig. S7, B and C). We conclude that whereas IRE1α and ATF6 likely play contributory roles toward cytoprotection, perhaps through cross-communication among the arms of the UPR, PERK signaling is centrally involved in mediating the cytoprotective effects of TERS priming. Our findings recognize PERK as the central facilitator of TERS-mediated cytoprotection.

To further validate this finding, we leveraged CRISPR/Cas9 (clustered regularly interspaced short palindromic repeats/CRISPR-associated protein 9) technology to target *ATF4*, which we found to be down-regulated during TERS priming (Figs. 2D and 3C). We designed guides targeting exon 2 of the *ATF4* gene using the px458 Cas9 plasmid (Fig. 6C). Transfected 293XT cells were positively sorted on the basis of GFP positivity. Selected clones were confirmed for deletion of the target exon by PCR blot analysis (Fig. 6D). *ATF4* deletion appeared to inhibit TERS-induced cytoprotection in recipient 293XT cells versus their wild-type counterparts (Fig. 6, E and F). Together, these data demonstrate that the UPR and particularly the PERK-ATF4 axis are necessary for TERS-mediated cytoprotection.

TERS-primed cells are more tumorigenic in vivo

Because TERS enabled cells to better cope with various noxae in culture, we hypothesized that TERS could provide cancer cells with growth advantage over naïve cancer cells in a coculture system. To this end, we tagged murine TC1 cells through stable transduction with a red fluorescent protein (RFP) gene driven by the cytomegalovirus promoter. Tagged or

untagged TC1 cells were then separately primed with TC1 Veh CM or TERS CM, respectively (Fig. 7A). The cell populations were then admixed and challenged with one of the following conditions: Tg, 2-deoxy-D-glucose, bortezomib, or paclitaxel. After a 24-hour challenge, we measured the relative percentage of live cells among RFP-positive versus RFP-negative cell populations. TERS-primed TC1 cells emerged as the prevalent cell population in each challenge condition (Fig. 7B). To control for any confounding factors due to ectopic RFP expression, priming conditions were reversed (meaning, TC1.RFP were TERS-primed and TC1 were vehicle-primed) and cocultured with identical challenges. We observed a similar trend (fig. S8). Thus, we conclude that TERS-primed cancer cells have a survival advantage over control cells, a conclusion that could bear considerable relevance to cell dynamics in the tumor microenvironment.

To test this possibility in vivo, we injected TERS- or vehicle-primed murine TC1 cells subcutaneously into C57BL/6mice. To eliminate host variability, TERS- and vehicle-primed cells were injected into opposite flanks of the same mouse. TERS-primed tumors became palpable on day 8, whereas control tumors emerged only after 14 days (Fig. 7C). On day 19 after injection, the average volume of TERS-primed tumors was substantially larger than that of vehicle-primed tumors. At sacrifice (day 30), tumors derived from TERS-primed cells were significantly greater in weight (Fig. 7D) and size (Fig. 7E) than those derived from vehicle-primed cells. Histological analysis, including hematoxylin and eosin (H&E) and Ki-67 staining, indicated no marked differences in morphology or proliferation between the two groups (fig. S9). Because TERS-primed cells had no proliferative advantage over vehicle-primed cells, as reflected in the lack of enrichment in G_1 phase (Fig. 4E) and Ki-67 staining (fig. S9), we conclude that the advantage of TERS-primed tumors over vehicle-primed tumors was the consequence of acquired adaptive fitness.

DISCUSSION

A UPR-based cell-nonautonomous regulation of tumorigenesis is an emerging concept in tumor biology and immunobiology (6, 18). This new idea stems from the observation that cancer cells experiencing a UPR release soluble factor(s) able to reproducibly transmit ER stress and elicit a UPR in $CD11b^+$ macrophages and dendritic cells (7–9, 55). Here, we demonstrate that a similar intercellular signaling event confers a prosurvival phenotype and clonal fitness to cancer cells upon challenge with microenvironmental and exogenous stressors.

One aspect of this TERS-induced phenotype was the initiation of Wnt signaling. β-Catenin is a central effector of the Wnt pathway and is involved in diverse cellular processes, including growth, differentiation, and transcription of Wnt-responsive genes (37, 38, 56), while driving the expression of several oncogenes, for example, *c-Myc, Cyclin D1*, and *Nos2* (57–59). TERS-mediated Wnt signaling activation required IRE1α. Because canonical ER stress conditions did not mimic this effect, we conclude that TERS-mediated Wnt signaling activation is unique. Although Wnt signaling driven by recombinant WNT provided cytoprotective effects during nutrient starvation, this phenomenon may be independent from, or unrelated to, TERS-mediated cytoprotection. The full interaction and dynamics of the TERS/Wnt pathways remain to be fully elucidated. Wnt signaling was

recently shown to occur in circulating prostate cancer cells of patients with antiandrogen resistance (60).

A salient finding of our study is the marked decrease in PERK-ATF4 activation in TERS-primed cells. Although unexpected, this finding provided a possible clue into the mechanism of cytoprotection. The activation of the PERK pathway leads to the transcription and translation of ATF4, which itself coordinates the activation of the downstream target CHOP to drive apoptosis (3). Here, we show that in TERS-primed cells, this classical cascade of events was substantially decreased because TERS-primed cells subject to nutrient deprivation or bortezomib treatment showed a pattern of ATF4 and downstream CHOP reduction. Although it has been reported that ATF4 can be regulated independently of the stress response (61), our data support a central role of the PERK-ATF4 axis in TERS-induced cellular fitness. In this context, we found that the prosurvival adaptive response to TERS required the attenuation of PERK and ATF4 activation, an effect lost through the deletion of the *PERK* or *ATF4* genes. Arguably, TERS may fine-tune ATF4 to promote cytoprotection. In support of our conclusion, mild ER stress conditions were reported to promote the degradation of two downstream ATF4 targets, CHOP and GADD34, and lead to cellular adaptation and survival (26). A slow translation of ATF4 was found to confer cytoprotection (62), presumably by preventing the activation of CHOP. Thus, because ATF4 can exert opposing roles in controlling cell fate (survival versus apoptosis), depending on its state of activation and abundance, we view ATF4 as a cellular rheostat able to gauge the effects of TERS in receiver cancer cells.

Other effects may also contribute to cytoprotection in TERS-primed cells. One possibility is the progressive increase in surface expression of GRP78 induced by TERS priming. GRP78 is considered the master regulator of the UPR (63, 64) and has been directly implicated in tumor progression in murine models of cancer (11, 65, 66). High levels of GRP78 predict poor prognosis in a variety of carcinoma (67), the development of therapy resistance, and cancer recurrence (68). GRP78 surface expression, although a relatively less characterized phenomenon (23, 69), has been shown to mediate growth signals for cancer cells through PI3K/AKT signaling and promote chemoresistance (15, 16, 70). Because surface relocalization of GRP78 was not associated with increased transcription, it is possible that TERS signaling induces posttranslational modifications of GRP78 to improve its overall function and stability, for instance, through AMPylation of Thr^{518} (71). A mild adaptive UPR promotes GRP78 protein half-life stability while not affecting its gene transcription (26). This demonstrates that some UPR-driven stimuli favor the stabilization of GRP78, as we observed in our durability experiments (Fig. 3, E and F). The abundance of the GRP78 chaperone would allow cells to better cope with subsequent pressures. Thus, a second possibility is that TERS-induced adaptive fitness reflects a stable level of chaperones. A final alternative mechanism to explain cytoprotection is TERT, which we found to accumulate in the cytoplasm. Through its noncanonical functions (72), TERT protects cells from apoptosis, enhances genomic stability and DNA repair (73), and attenuates ER stress–induced cell death (48). The mechanisms of TERS on receiver cells discussed above are summarized in the model shown in Fig. 8.

The cell-extrinsic effects of the tumor UPR represent a novel mechanism through which cancer cells adapt to tumor microenvironmental noxae (hypoxia, nutrient starvation, biosynthetic errors, and viral infection) and apoptosis-inducing chemotherapeutic agents. An unresolved aspect of our work concerns the exact chemical nature and identity of TERS. Undergoing studies show that TERS is present at markedly low abundance in cancer cell CM, making it particularly arduous to isolate to purity. Recent reports emphasized the role of by-products of lipid oxidation (74, 75) as responsible actors in phenomena closely related to TERS. However, we have verified that, by mass spectrometry and bioactivity assays, TERS is not the products claimed in these reports but is instead a unique factor yet to be conclusively isolated. Although work on the final identification of TERS is continuing, the results of the present study show that a UPR-based cell-nonautonomous regulation among cancer cells endows receiver cells with cellular fitness by exerting a selective pressure. Because cytoprotection is relatively durable, one can also predict that daughter cells of the initial receiver cells may also be protected, suggesting that TERS may have epigenetic consequences on target cells. In light of the unique regulation of both UPR- and Wnt-related genes, it is likely that TERS affects other cellular processes, such as autophagy, which may also bolster cell survival. Notably, TERS-primed cells did not have a proliferative advantage over vehicle-primed cells but rather a fitness advantage. Therefore, the persistence of a TERS-primed population within the tumor microenvironment may lay dormant until a new selective pressure initiates the emergence of the fittest clones.

Our findings corroborate the conclusions of recent reports that showed that individual tumor cells within a uniform genetic lineage can acquire functionally different behaviors in vivo, implying that functional clonal diversity may reflect the outgrowth of cells with greater fitness and extended survival generated by cell-nonautonomous signaling and processes (76, 77). Accordingly, future management of cancer should take into consideration these new aspects of cancer cell dynamics within the tumor microenvironment.

MATERIALS AND METHODS

Cell lines and cell culture

PC3, LNCaP, DU145, and TC1 prostate cancer cells and 293XT cells were grown in RPMI or Dulbecco's modified Eagle's medium (DMEM) (Corning) supplemented with 10% FBS (HyClone) and 1% penicillin/streptomycin/L-glutamine, nonessential amino acids, sodium pyruvate, and HEPES (cDMEM). All cell lines were maintained at 37°C in 5% CO_2O_2. All cell lines were mycoplasma-free as determined by PCR assay (SouthernBiotech). MEF lines (gift from J. Lin) were previously derived and described: PERK KO (78), IRE1α KO (79), and ATF6 KO (80). They were cultured under standard cDMEM conditions.

TERS CM generation

Transmitting cells as specified in each experiment were induced to undergo ER stress through treatment with Tg (300 nM) (Enzo Life Sciences) for 2 hours. Control cells were similarly treated with an equal volume of vehicle (0.02% EtOH). Cells were washed twice with Dulbecco's phosphate-buffered saline (PBS) (Corning) and then incubated in fresh, standard growth medium for 16 hours. CM was then harvested, centrifuged for 10 min at

2000 rpm, filtered through a 0.22-μm filter (Millipore), and used to treat cells. For TERS priming, CM was generated from homologous cells unless otherwise specified.

Nutrient starvation studies

To create nutrient starvation conditions, cells were washed two times with PBS and cultured in glucose-free DMEM (Gibco) supplemented only with 1% penicillin/streptomycin.

Reverse transcription quantitative polymerase chain reaction

RNA was harvested from cells using the NucleoSpin II Kit (Macherey-Nagel). The concentration and purity of RNA were quantified on a NanoDrop (ND-1000) spectrophotometer (Thermo Scientific) and analyzed with NanoDrop software version 3.8.0. RNA was normalized between conditions, and complementary DNA (cDNA) was generated using a High-Capacity cDNA Synthesis kit (Life Technologies). RT-qPCR was performed on an ABI 7300 Real-Time PCR system using TaqMan reagents for 50 cycles under universal cycling conditions according to the manufacturer's specifications (Kapa Biosystems). Target gene expression was normalized to β-*actin*, and relative expression was determined using the $-\Delta\Delta C_t$ relative quantification method. Validated FAM-labeled human *HSPA5* (GRP78) (catalog no. Hs00607129_gH, Life Technologies), *XBP-1s* (forward: 5′-CCGCAGCAGGTGCAGG-3′; reverse: 5′-GAGTCAATACCGCCAGAATCCA-3′) (Integrated DNA Technologies), *DDIT3* (CHOP) (catalog no. Hs00358796_g1, Life Technologies), *IL-6* (catalog no. Hs00985639_m1, Life Technologies), *CTNNB1* (β-catenin) (catalog no. Hs00355049_m1, Life Technologies), *AXIN2* (forward: 5′-GACAGTGAGATATCCAGTGATGC-3′; reverse: 5′-GTTTCTTACTGCCCACACGATA-3′) (Integrated DNA Technologies), *hTERT* (forward: 5′-CGGTTGAAGGTGAGACTGG-3′; reverse: 5′-GCACGGCTTTTGTTCAGATG-3′) (Integrated DNA Technologies), and VIC-labeled human β-*actin* TaqMan primer/probe sets (catalog no. 4326315E, Life Technologies) were used.

Flow cytometry

Apoptosis assays were performed on single-cell suspensions, stained with fluorescein isothiocyanate (FITC)–conjugated annexin V and PI using the FITC Annexin V Apoptosis Detection Kit (BD Biosciences). Data were acquired on a FACSCalibur flow cytometer (BD Biosciences) and analyzed using CellQuest Pro (BD Biosciences) and FlowJo software (Tree Star). For sGRP78 detection, single-cell suspensions were washed once with PBS and then stained with goat polyclonal antibody to surface-expressed human GRP78 (catalog no. SC-1051, Santa Cruz Biotechnology). Cells were then washed with PBS and counterstained with FITC-labeled donkey polyclonal antibody to goat immunoglobulin (Ig) (Santa Cruz Biotechnology). Stained cells were washed again with PBS and resuspended in 7AAD staining buffer and analyzed by flow cytometry by 7AAD exclusion. Cell cycle analysis was performed using FITC-BrdU Flow Kit (BD Biosciences) per the manufacturer's protocol.

TOP reporter system

Lentiviral TOP-GFP construct was previously described (42) and was a gift from K. Willert. PC3 cells were transduced with lentivirus supplemented with polybrene (4 μg/ml; Sigma) for

48 hours. After incubation, cells were cultured in standard growth medium for 24 hours. Positively transduced cells were selected under puromycin (1 μg/ml) for 2 weeks. PC3.TOP cells were then treated as described and analyzed for TOP activity using a FACSCalibur flow cytometer probing for GFP expression on 7AAD-negative cells. Stimulation of PC3.TOP cells with rWNT3a (20 ng/ml; HumanZyme) was performed for 48 hours. UPR inhibitors 4μ8C (Axon MedChem) and GSK2656157 (Selleckchem) were used at the dose indicated in Fig. 5.

Promoter activity assays

The TERT core promoter luciferase construct was previously designed (50) through the insertion of wild-type promoter sequence into the pGL4.10 (Promega) vector and was a gift from J. Costello (University of California, San Francisco). The ATF6 luciferase reporter construct was previously designed (80) and was provided by J. Lin. Cells were transiently transfected for 18 hours with Lipofectamine 3000 (Thermo Fisher) with either the TERT or the ATF6 promoter construct. For normalization control, cells were concomitantly transfected with a *Renilla* plasmid driven by the TK promoter (Promega). Transiently transfected cells were washed, treated as specified in the text, and subsequently analyzed for luciferase and *Renilla* expression using the Dual-Luciferase Reporter Assay (Promega) according to the manufacturer's protocol.

Confocal microscopy

Cells were plated on glass slides in a tissue culture plate and treated as specified in Figs. 1, 4, and 5. After treatment, the medium was gently removed by aspiration. Cells were then washed with cold PBS and fixed using 4% formaldehyde (Fisher Scientific) for 15 min. The formaldehyde solution was gently removed by aspiration, and the cells were washed three times with PBS. The fixed cells were then blocked/permeabilized with 5% bovine serum albumin (BSA) (Fisher Scientific) and 0.3% Triton X-100 (Fisher Scientific) in PBS for 1 hour. Cells were washed three times with PBS and then probed with antibodies to hTERT (catalog no. SC7215, Santa Cruz Biotechnology), β-catenin (catalog no. 8480P, Cell Signaling Technology), or GRP78 (catalog no. SC-1050, Santa Cruz Biotechnology) by incubating at the manufacturer's recommended dilution in PBS-BSA at 4°C overnight. After incubation with the primary antibody, cells were washed three times with PBS and counterstained with an FITC-conjugated antibody as follows: polyclonal donkey antibody to goat Ig (Santa Cruz Biotechnology) for hTERT or polyclonal goat antibody to rabbit Ig (Biomeda) for β-catenin and GRP78, in the dark for 1 hour. Cells were then washed three times with PBS and mounted onto microscope slides using the ProLong Gold Antifade Reagent with 4′,6-diamidino-2-phenylindole (Invitrogen). Once mounted, the slides were imaged using a BIOREVO BZ-9000 microscope or a Zeiss LSM 510 laser scanning confocal microscope at the University of California at San Diego (UCSD) Microscopy Core. Staining for γ-H2AX was performed according to (81).

Western blot analysis

After treatment, PC3, DU145, or LNCaP cells were washed with ice-cold PBS and suspended in radioimmunoprecipitation assay (RIPA) lysis buffer: 1× RIPA buffer and a cocktail of protease inhibitors (Santa Cruz Biotechnology). Cell lysates were centrifuged at

16,000*g* for 15 min, and the supernatants were collected. Protein concentration was determined using the Pierce BCA Protein Assay Kit (Thermo Scientific). Samples were heat-denatured, and equal concentrations of protein were loaded onto a 4 to 20% Mini-PROTEAN TGX Precast Gels (Bio-Rad), electrophoresed, and transferred onto 0.2-μm polyvinylidene difluoride membrane in tris-glycine transfer buffer containing 20% methanol. The membranes were then blocked with 5% nonfat milk in tris-buffered saline (TBS) containing 0.1% Tween 20 (TBS-T) for 1 hour at room temperature. The membranes were then incubated with the specified primary antibodies overnight at 4°C. Membranes were washed for 5 min at room temperature three times by TBS-T, incubated with a horseradish peroxidase (HRP)–labeled secondary antibody in 5% nonfat milk for 1 hour at room temperature, and washed for 5 min at room temperature three times in TBS-T. Bound antibodies were detected by chemiluminescence reaction using Pierce ECL Blotting Substrate (Thermo Scientific). The following primary antibodies were used: mouse monoclonal antibody to human GRP78 (BD Biosciences), rabbit monoclonal antibody to human PERK (Cell Signaling Technology), rabbit monoclonal antibody to phospho-eIF2α (Ser^{51}) (Cell Signaling Technology), rabbit polyclonal antibodies to human ATF4 (CREB-2) (Santa Cruz Biotechnology), mouse monoclonal antibody to human CHOP (GADD153) (Santa Cruz Biotechnology), rabbit polyclonal antibodies to human HSP90 (GeneTex), and HRP-conjugated goat antibodies to β-actin (Santa Cruz Biotechnology). Secondary antibodies were HRP-conjugated anti-mouse IgG or anti-rabbit IgG (Santa Cruz Biotechnology).

Cell tagging

The tRFP (tag red fluorescent protein) cDNA was amplified from pTRIPZ plasmid (Open Biosystems) by PCR using a specific primer (forward: 5′-ttggtaccgagctcggatccGCCACCATGAGCGAGCTG-3′; reverse: 5′-ccctctagatgcatgctcgagTTATCTGTGCCCCAGTTTGC-3′). The amplified tRFP fragment was purified by agarose gel and assembled with pLPC-puro retrovirus vector digested with Hind III and Xho I using the Gibson Assembly Master Mix (New England Biolabs). For retrovirus packaging, Phoenix-Ampho cells in a 10-cm dish were transfected with 10 μg of plasmid using PEI-Max (1 μg/μl; Polysciences Inc.), and the supernatant containing retrovirus particles was collected at 48 and 72 hours after transfection. TC1 cells were retrovirally transduced with tRFP using polybrene (8 μg/ml). Puromycin selection was initiated 2 days after transduction, and cells were maintained in the presence of puromycin (5 μg/ml) until use.

In vivo studies

TC1 cells were primed with Veh CM or TERS CM. Cells were enzymatically detached from plastic and resuspended in PBS at a final concentration of 5×10^6 cells/ml. C57BL/6 mice were injected with 100 μl of vehicle cell suspension into the left flank and 100 μl of TERS-primed cells in the contralateral right flank. Mice were initially monitored for tumor take by palpation. When tumors became palpable, tumor size was determined through two-dimensional caliper measurements every 3 days. Mice were sacrificed when a tumor reached 20 mm in any one dimension, per UCSD animal welfare standards, or at 30 days after implantation. Tumor volume was calculated using the following ellipsoid formula: $V = ½(H$

$\times W^2$). Upon mouse sacrifice, tumors were resected. For histological analysis, tumors were frozen in optimum cutting temperature compound and processed at the UCSD histology core, and stained for Ki-67 or H&E.

CRISPR/Cas9 studies

Two pairs of Cas9 guides were designed using the CHOPCHOP (82) software (available at http://chopchop.cbu.uib.no/). The sequences for guide 1 were caccgGCAACGTAAGCAGTGTAGTC (forward) and aaacGACTACACTGCTTACGTTGCc (reverse), and the sequences for guide 2 were caccgGGATTTGAAGGAGTTCGACT (forward) and aaacAGTCGAACTCCTTCAAATCCc (reverse) (lowercase letters indicate overhangs). Guides were cloned into the SpCas9-2A-GFP (px458) backbone modified to contain an eIF1α promoter (px458-ef1a) (83). Px458 was a gift from F. Zhang (Addgene plasmid #48138). Briefly, Cas9 guides were then purchased as oligonucleotides from Integrated DNA Technologies. These oligonucleotide guide pairs were phosphorylated, annealed, and ligated into Bbs I–digested px458 backbone. The ligated plasmid was then transformed into DH5α bacteria and grown on carbenicillin plates overnight at 37°C. Single colonies were picked and cultured overnight, the plasmids were isolated by Miniprep or Midiprep (Invitrogen), and the sequence was validated. 293XT cells were grown in DMEM with 10% FBS. Twenty-four hours before transfection with the guide-containing px458-ef1a plasmids (using Lipofectamine 3000), 8×10^4 cells/cm^2 were seeded onto six-well plates. Three days after transfection, cells were sorted by fluorescence-activated cell sorting on the basis of GFP positivity. Cells were then cultured in DMEM with 10% FBS for at least 1 week, validated, and used in TERS priming experiments. To demonstrate Cas9 efficiency, genomic DNA was isolated and PCR-amplified using GoTaq (Promega) according to the manufacturer's instructions. The PCR product was then resolved on a 0.8% agarose gel and imaged under ultraviolet light.

Supplementary Material

Refer to Web version on PubMed Central for supplementary material.

Acknowledgments

We thank J. Costello (University of California, San Francisco) for providing the TERT core promoter luciferase construct; J. Lin (UCSD) for the ATF6 luciferase reporter; K. Willert (UCSD) for providing the lentiviral TOP-GFP construct; and F. Zhang for the Addgene px458 plasmid.

Funding: This work was supported by U.S. Department of Defense grant W81XWH-12-1-0156 to M.Z. and NIH R01NS088485, NIH U54OD020351, and VA BX002284 to J.H.L. J.J.R. acknowledges the support of the Frank H. and Eva B. Buck Foundation. N.H. was supported by a Japan Society for the Promotion of Science Postdoctoral Fellowship for Research Abroad.

References

1. Heazlewood CK, Cook MC, Eri R, Price GR, Tauro SB, Taupin D, Thornton DJ, Png CW, Crockford TL, Cornall RJ, Adams R, Kato M, Nelms KA, Hong NA, Florin THJ, Goodnow CC, McGuckin MA. Aberrant mucin assembly in mice causes endoplasmic reticulum stress and spontaneous inflammation resembling ulcerative colitis. PLOS Med. 2008; 5:e54. [PubMed: 18318598]

2. He B. Viruses, endoplasmic reticulum stress, and interferon responses. Cell Death Differ. 2006; 13:393–403. [PubMed: 16397582]
3. Walter P, Ron D. The unfolded protein response: From stress pathway to homeostatic regulation. Science. 2011; 334:1081–1086. [PubMed: 22116877]
4. Yamamoto K, Sato T, Matsui T, Sato M, Okada T, Yoshida H, Harada A, Mori K. Transcriptional induction of mammalian ER quality control proteins is mediated by single or combined action of ATF6α and XBP1. Dev. Cell. 2007; 13:365–376. [PubMed: 17765680]
5. Zinszner H, Kuroda M, Wang X, Batchvarova N, Lightfoot RT, Remotti H, Stevens JL, Ron D. CHOP is implicated in programmed cell death in response to impaired function of the endoplasmic reticulum. Genes Dev. 1998; 12:982–995. [PubMed: 9531536]
6. Mahadevan NR, Zanetti M. Tumor stress inside out: Cell-extrinsic effects of the unfolded protein response in tumor cells modulate the immunological landscape of the tumor microenvironment. J. Immunol. 2011; 187:4403–4409. [PubMed: 22013206]
7. Mahadevan NR, Rodvold J, Sepulveda H, Rossi S, Drew AF, Zanetti M. Transmission of endoplasmic reticulum stress and pro-inflammation from tumor cells to myeloid cells. Proc. Natl. Acad. Sci. U.S.A. 2011; 108:6561–6566. [PubMed: 21464300]
8. Mahadevan NR, Anufreichik V, Rodvold JJ, Chiu KT, Sepulveda H, Zanetti M. Cell-extrinsic effects of tumor ER stress imprint myeloid dendritic cells and impair $CD8^+$ T cell priming. PLOS ONE. 2012; 7:e51845. [PubMed: 23272178]
9. Cullen SJ, Fatemie S, Ladiges W. Breast tumor cells primed by endoplasmic reticulum stress remodel macrophage phenotype. Am. J. Cancer Res. 2013; 3:196–210. [PubMed: 23593541]
10. Rodvold JJ, Mahadevan NR, Zanetti M. Immune modulation by ER stress and inflammation in the tumor microenvironment. Cancer Lett. 2015; 380:227–236. [PubMed: 26525580]
11. Fu Y, Wey S, Wang M, Ye R, Liao C-P, Roy-Burman P, Lee AS. Pten null prostate tumorigenesis and AKT activation are blocked by targeted knockout of ER chaperone GRP78/BiP in prostate epithelium. Proc. Natl. Acad. Sci. U.S.A. 2008; 105:19444–19449. [PubMed: 19033462]
12. Bi M, Naczki C, Koritzinsky M, Fels D, Blais J, Hu N, Harding H, Novoa I, Varia M, Raleigh J, Scheuner D, Kaufman RJ, Bell J, Ron D, Wouters BG, Koumenis C. ER stress-regulated translation increases tolerance to extreme hypoxia and promotes tumor growth. EMBO J. 2005; 24:3470–3481. [PubMed: 16148948]
13. Li J, Lee AS. Stress induction of GRP78/BiP and its role in cancer. Curr. Mol. Med. 2006; 6:45–54. [PubMed: 16472112]
14. Ranganathan AC, Zhang L, Adam AP, Aguirre-Ghiso JA. Functional coupling of p38-induced up-regulation of BiP and activation of RNA-dependent protein kinase–like endoplasmic reticulum kinase to drug resistance of dormant carcinoma cells. Cancer Res. 2006; 66:1702–1711. [PubMed: 16452230]
15. Misra UK, Deedwania R, Pizzo SV. Activation and cross-talk between Akt, NF-κB, and unfolded protein response signaling in 1-LN prostate cancer cells consequent to ligation of cell surface-associated GRP78. J. Biol. Chem. 2006; 281:13694–13707. [PubMed: 16543232]
16. Zhang Y, Tseng C-C, Tsai Y-L, Fu X, Schiff R, Lee AS. Cancer cells resistant to therapy promote cell surface relocalization of GRP78 which complexes with PI3K and enhances PI(3,4,5)P3 production. PLOS ONE. 2013; 8:e80071. [PubMed: 24244613]
17. Taylor RC, Dillin A. XBP-1 is a cell-nonautonomous regulator of stress resistance and longevity. Cell. 2013; 153:1435–1447. [PubMed: 23791175]
18. Zanetti M, Rodvold JJ, Mahadevan NR. The evolving paradigm of cell-nonautonomous UPR-based regulation of immunity by cancer cells. Oncogene. 2015; 35:269–278. [PubMed: 25893303]
19. Spiotto MT, Banh A, Papandreou I, Cao H, Galvez MG, Gurtner GC, Denko NC, Le QT, Koong AC. Imaging the unfolded protein response in primary tumors reveals microenvironments with metabolic variations that predict tumor growth. Cancer Res. 2010; 70:78–88. [PubMed: 20028872]
20. Arap MA, Lahdenranta J, Mintz PJ, Hajitou A, Sarkis AS, Arap W, Pasqualini R. Cell surface expression of the stress response chaperone GRP78 enables tumor targeting by circulating ligands. Cancer Cell. 2004; 6:275–284. [PubMed: 15380518]

21. Ray R, de Ridder GG, Eu JP, Paton AW, Paton JC, Pizzo SV. The *Escherichia coli* subtilase cytotoxin A subunit specifically cleaves cell-surface GRP78 protein and abolishes COOH-terminal-dependent signaling. J. Biol. Chem. 2012; 287:32755–32769. [PubMed: 22851173]
22. Grivennikov SI, Greten FR, Karin M. Immunity, inflammation, and cancer. Cell. 2010; 140:883–899. [PubMed: 20303878]
23. Ni M, Zhang Y, Lee AS. Beyond the endoplasmic reticulum: Atypical GRP78 in cell viability, signalling and therapeutic targeting. Biochem. J. 2011; 434:181–188. [PubMed: 21309747]
24. Quinones QJ, de Ridder GG, Pizzo SV. GRP78: A chaperone with diverse roles beyond the endoplasmic reticulum. Histol. Histopathol. 2008; 23:1409–1416. [PubMed: 18785123]
25. Shin BK, Wang H, Yim AM, Le Naour F, Brichory F, Jang JH, Zhao R, Puravs E, Tra J, Michael CW, Misek DE, Hanash SM. Global profiling of the cell surface proteome of cancer cells uncovers an abundance of proteins with chaperone function. J. Biol. Chem. 2003; 278:7607–7616. [PubMed: 12493773]
26. Rutkowski DT, Arnold SM, Miller CN, Wu J, Li J, Gunnison KM, Mori K, Sadighi Akha AA, Raden D, Kaufman RJ. Adaptation to ER stress is mediated by differential stabilities of pro-survival and pro-apoptotic mRNAs and proteins. PLOS Biol. 2006; 4:e374. [PubMed: 17090218]
27. Richardson PG, Sonneveld P, Schuster MW, Irwin D, Stadtmauer EA, Facon T, Harousseau J-L, Ben-Yehuda D, Lonial S, Goldschmidt H, Reece D, San-Miguel JF, Bladé J, Boccadoro M, Cavenagh J, Dalton WS, Boral AL, Esseltine DL, Porter JB, Schenkein D, Anderson KC. Assessment of Proteasome Inhibition for Extending Remissions (APEX) Investigators, Bortezomib or high-dose dexamethasone for relapsed multiple myeloma. N. Engl. J. Med. 2005; 352:2487–2498. [PubMed: 15958804]
28. Papandreou CN, Daliani DD, Nix D, Yang H, Madden T, Wang X, Pien CS, Millikan RE, Tu S-M, Pagliaro L, Kim J, Adams J, Elliott P, Esseltine D, Petrusich A, Dieringer P, Perez C, Logothetis CJ. Phase I trial of the proteasome inhibitor bortezomib in patients with advanced solid tumors with observations in androgen-independent prostate cancer. J. Clin. Oncol. 2004; 22:2108–2121. [PubMed: 15169797]
29. Papandreou CN, Logothetis CJ. Bortezomib as a potential treatment for prostate cancer. Cancer Res. 2004; 64:5036–5043. [PubMed: 15289299]
30. Lee A-H, Iwakoshi NN, Anderson KC, Glimcher LH. Proteasome inhibitors disrupt the unfolded protein response in myeloma cells. Proc. Natl. Acad. Sci. U.S.A. 2003; 100:9946–9951. [PubMed: 12902539]
31. Armstrong JL, Flockhart R, Veal GJ, Lovat PE, Redfern CPF. Regulation of endoplasmic reticulum stress-induced cell death by ATF4 in neuroectodermal tumor cells. J. Biol. Chem. 2010; 285:6091–6100. [PubMed: 20022965]
32. Jeon YJ, Khelifa S, Ratnikov B, Scott DA, Feng Y, Parisi F, Ruller C, Lau E, Kim H, Brill LM, Jiang T, Rimm DL, Cardiff RD, Mills GB, Smith JW, Osterman AL, Kluger Y, Ronai ZA. Regulation of glutamine carrier proteins by RNF5 determines breast cancer response to ER stress-inducing chemotherapies. Cancer Cell. 2015; 27:354–369. [PubMed: 25759021]
33. Jordan MA, Toso RJ, Thrower D, Wilson L. Mechanism of mitotic block and inhibition of cell proliferation by taxol at low concentrations. Proc. Natl. Acad. Sci. U.S.A. 1993; 90:9552–9556. [PubMed: 8105478]
34. Woods CM, Zhu J, McQueney PA, Bollag D, Lazarides E. Taxol-induced mitotic block triggers rapid onset of a p53-independent apoptotic pathway. Mol. Med. 1995; 1:506–526. [PubMed: 8529117]
35. DiPaola RS. To arrest or not to G_2-M cell-cycle arrest: Commentary re: A. K. Tyagi *et al.*, Silibinin strongly synergizes human prostate carcinoma DU145 cells to doxorubicin-induced growth inhibition, G_2-M arrest, and apoptosis. Clin. Cancer Res., 8: 3512–3519, 2002. Clin. Cancer. Res. 2002; 8:3311–3314. [PubMed: 12429616]
36. Davidson G, Niehrs C. Emerging links between CDK cell cycle regulators and Wnt signaling. Trends Cell Biol. 2010; 20:453–460. [PubMed: 20627573]
37. Willert K, Nusse R. β-Catenin: A key mediator of Wnt signaling. Curr. Opin. Genet. Dev. 1998; 8:95–102. [PubMed: 9529612]

38. Clevers H, Nusse R. Wnt/β-catenin signaling and disease. Cell. 2012; 149:1192–1205. [PubMed: 22682243]
39. Ikeda S, Kishida S, Yamamoto H, Murai H, Koyama S, Kikuchi A. Axin, a negative regulator of the Wnt signaling pathway, forms a complex with GSK-3β and β-catenin and promotes GSK-3β-dependent phosphorylation of β-catenin. EMBO J. 1998; 17:1371–1384. [PubMed: 9482734]
40. Veeman MT, Slusarski DC, Kaykas A, Louie SH, Moon RT. Zebrafish prickle, a modulator of noncanonical Wnt/Fz signaling, regulates gastrulation movements. Curr. Biol. 2003; 13:680–685. [PubMed: 12699626]
41. Fuerer C, Nusse R. Lentiviral vectors to probe and manipulate the Wnt signaling pathway. PLOS ONE. 2010; 5:e9370. [PubMed: 20186325]
42. Fernandez A, Huggins IJ, Perna L, Brafman D, Lu D, Yao S, Gaasterland T, Carson DA, Willert K. The WNT receptor FZD7 is required for maintenance of the pluripotent state in human embryonic stem cells. Proc. Natl. Acad. Sci. U.S.A. 2014; 111:1409–1414. [PubMed: 24474766]
43. Atilla-Gokcumen GE, Williams DS, Bregman H, Pagano N, Meggers E. Organometallic compounds with biological activity: A very selective and highly potent cellular inhibitor for glycogen synthase kinase 3. Chembiochem. 2006; 7:1443–1450. [PubMed: 16858717]
44. Logan CY, Nusse R. The Wnt signaling pathway in development and disease. Annu. Rev. Cell Dev. Biol. 2004; 20:781–810. [PubMed: 15473860]
45. Cross BCS, Bond PJ, Sadowski PG, Jha BK, Zak J, Goodman JM, Silverman RH, Neubert TA, Baxendale IR, Ron D, Harding HP. The molecular basis for selective inhibition of unconventional mRNA splicing by an IRE1-binding small molecule. Proc. Natl. Acad. Sci. U.S.A. 2012; 109:E869–E878. [PubMed: 22315414]
46. Axten JM, Romeril SP, Shu A, Ralph J, Medina JR, Feng Y, Li WHH, Grant SW, Heerding DA, Minthorn E, Mencken T, Gaul N, Goetz A, Stanley T, Hassell AM, Gampe RT, Atkins C, Kumar R. Discovery of GSK2656157: An optimized PERK inhibitor selected for preclinical development. ACS Med. Chem. Lett. 2013; 4:964–968. [PubMed: 24900593]
47. Hoffmeyer K, Raggioli A, Rudloff S, Anton R, Hierholzer A, Del Valle I, Hein K, Vogt R, Kemler R. Wnt/β-catenin signaling regulates telomerase in stem cells and cancer cells. Science. 2012; 336:1549–1554. [PubMed: 22723415]
48. Hosoi T, Inoue Y, Nakatsu K, Matsushima N, Kiyose N, Shimamoto A, Tahara H, Ozawa K. TERT attenuated ER stress-induced cell death. Biochem. Biophys. Res. Commun. 2014; 447:378–382. [PubMed: 24746472]
49. Zhou J, Mao B, Zhou Q, Ding D, Wang M, Guo P, Gao Y, Shay JW, Yuan Z, Cong Y-S. Endoplasmic reticulum stress activates telomerase. Aging Cell. 2014; 13:197–200. [PubMed: 24119029]
50. Bell RJ, Rube HT, Kreig A, Mancini A, Fouse SD, Nagarajan RP, Choi S, Hong C, He D, Pekmezci M, Wiencke JK, Wrensch MR, Chang SM, Walsh KM, Myong S, Song JS, Costello JF. The transcription factor GABP selectively binds and activates the mutant TERT promoter in cancer. Science. 2015; 348:1036–1039. [PubMed: 25977370]
51. Haendeler J, Hoffmann J, Brandes RP, Zeiher AM, Dimmeler S. Hydrogen peroxide triggers nuclear export of telomerase reverse transcriptase via Src kinase family-dependent phosphorylation of tyrosine 707. Mol. Cell Biol. 2003; 23:4598–4610. [PubMed: 12808100]
52. B'chir W, Maurin A-C, Carraro V, Averous J, Jousse C, Muranishi Y, Parry L, Stepien G, Fafournoux P, Bruhat A. The eIF2α/ATF4 pathway is essential for stress-induced autophagy gene expression. Nucleic Acids Res. 2013; 41:7683–7699. [PubMed: 23804767]
53. Ye J, Kumanova M, Hart LS, Sloane K, Zhang H, De Panis DN, Bobrovnikova-Marjon E, Diehl JA, Ron D, Koumenis C. The GCN2-ATF4 pathway is critical for tumour cell survival and proliferation in response to nutrient deprivation. EMBO J. 2010; 29:2082–2096. [PubMed: 20473272]
54. Notte A, Rebucci M, Fransolet M, Roegiers E, Genin M, Tellier C, Watillon K, Fattaccioli A, Arnould T, Michiels C. Taxol-induced unfolded protein response activation in breast cancer cells exposed to hypoxia: ATF4 activation regulates autophagy and inhibits apoptosis. Int. J. Biochem. Cell Biol. 2015; 62:1–14. [PubMed: 25724736]

55. Condamine T, Kumar V, Ramachandran IR, Youn J-I, Celis E, Finnberg N, El-Deiry WS, Winograd R, Vonderheide RH, English NR, Knight SC, Yagita H, McCaffrey JC, Antonia S, Hockstein N, Witt R, Masters G, Bauer T, Gabrilovich DI. ER stress regulates myeloid-derived suppressor cell fate through TRAIL-R-mediated apoptosis. J. Clin. Invest. 2014; 124:2626–2639. [PubMed: 24789911]
56. Nusse R, Fuerer C, Ching W, Harnish K, Logan C, Zeng A, ten Berge D, Kalani Y. Wnt signaling and stem cell control. Cold Spring Harb. Symp. Quant. Biol. 2008; 73:59–66. [PubMed: 19028988]
57. He TC, Sparks AB, Rago C, Hermeking H, Zawel L, da Costa LT, Morin PJ, Vogelstein B, Kinzler KW. Identification of c-*MYC* as a target of the APC pathway. Science. 1998; 281:1509–1512. [PubMed: 9727977]
58. Tetsu O, McCormick F. β-Catenin regulates expression of cyclin D1 in colon carcinoma cells. Nature. 1999; 398:422–426. [PubMed: 10201372]
59. Du Q, Park KS, Guo Z, He P, Nagashima M, Shao L, Sahai R, Geller DA, Hussain SP. Regulation of human nitric oxide synthase 2 expression by Wnt β-catenin signaling. Cancer Res. 2006; 66:7024–7031. [PubMed: 16849547]
60. Miyamoto DT, Zheng Y, Wittner BS, Lee RJ, Zhu H, Broderick KT, Desai R, Fox DB, Brannigan BW, Trautwein J, Arora KS, Desai N, Dahl DM, Sequist LV, Smith MR, Kapur R, Wu C-L, Shioda T, Ramaswamy S, Ting DT, Toner M, Maheswaran S, Haber DA. RNA-seq of single prostate CTCs implicates noncanonical Wnt signaling in antiandrogen resistance. Science. 2015; 349:1351–1356. [PubMed: 26383955]
61. Ben-Sahra I, Hoxhaj G, Ricoult SJH, Asara JM, Manning BD. mTORC1 induces purine synthesis through control of the mitochondrial tetrahydrofolate cycle. Science. 2016; 351:728–733. [PubMed: 26912861]
62. Walter F, Schmid J, Düssmann H, Concannon CG, Prehn JHM. Imaging of single cell responses to ER stress indicates that the relative dynamics of IRE1/XBP1 and PERK/ATF4 signalling rather than a switch between signalling branches determine cell survival. Cell Death Differ. 2015; 22:1502–1516. [PubMed: 25633195]
63. Bertolotti A, Zhang Y, Hendershot LM, Harding HP, Ron D. Dynamic interaction of BiP and ER stress transducers in the unfolded-protein response. Nat. Cell Biol. 2000; 2:326–332. [PubMed: 10854322]
64. Lee AS. Glucose-regulated proteins in cancer: Molecular mechanisms and therapeutic potential. Nat. Rev. Cancer. 2014; 14:263–276. [PubMed: 24658275]
65. Jamora C, Dennert G, Lee AS. Inhibition of tumor progression by suppression of stress protein GRP78/BiP induction in fibrosarcoma B/C10ME. Proc. Natl. Acad. Sci. U.S.A. 1996; 93:7690–7694. [PubMed: 8755537]
66. Dong D, Ni M, Li J, Xiong S, Ye W, Virrey JJ, Mao C, Ye R, Wang M, Pen L, Dubeau L, Groshen S, Hofman FM, Lee AS. Critical role of the stress chaperone GRP78/BiP in tumor proliferation, survival, and tumor angiogenesis in transgene-induced mammary tumor development. Cancer Res. 2008; 68:498–505. [PubMed: 18199545]
67. Lee AS. GRP78 induction in cancer: Therapeutic and prognostic implications. Cancer Res. 2007; 67:3496–3499. [PubMed: 17440054]
68. Daneshmand S, Quek ML, Lin E, Lee C, Cote RJ, Hawes D, Cai J, Groshen S, Lieskovsky G, Skinner DG, Lee AS, Pinski J. Glucose-regulated protein GRP78 is upregulated in prostate cancer and correlates with recurrence and survival. Hum. Pathol. 2007; 38:1547–1552. [PubMed: 17640713]
69. Gonzalez-Gronow M, Selim MA, Papalas J, Pizzo SV. GRP78: A multifunctional receptor on the cell surface. Antioxid. Redox Signal. 2009; 11:2299–2306. [PubMed: 19331544]
70. Gonzalez-Gronow M, Cuchacovich M, Llanos C, Urzua C, Gawdi G, Pizzo SV. Prostate cancer cell proliferation in vitro is modulated by antibodies against glucose-regulated protein 78 isolated from patient serum. Cancer Res. 2006; 66:11424–11431. [PubMed: 17145889]
71. Preissler S, Rato C, Chen R, Antrobus R, Ding S, Fearnley IM, Ron D. AMPylation matches BiP activity to client protein load in the endoplasmic reticulum. Elife. 2015; 4:e12621. [PubMed: 26673894]

72. Li Y, Tergaonkar V. Noncanonical functions of telomerase: Implications in telomerase-targeted cancer therapies. Cancer Res. 2014; 74:1639–1644. [PubMed: 24599132]

73. Sharma GG, Gupta A, Wang H, Scherthan H, Dhar S, Gandhi V, Iliakis G, Shay JW, Young CS, Pandita TK. hTERT associates with human telomeres and enhances genomic stability and DNA repair. Oncogene. 2003; 22:131–146. [PubMed: 12527915]

74. Cubillos-Ruiz JR, Silberman PC, Rutkowski MR, Chopra S, Perales-Puchalt A, Song M, Zhang S, Bettigole SE, Gupta D, Holcomb K, Ellenson LH, Caputo T, Lee A-H, Conejo-Garcia JR, Glimcher LH. ER stress sensor XBP1 controls anti-tumor immunity by disrupting dendritic cell homeostasis. Cell. 2015; 161:1527–1538. [PubMed: 26073941]

75. Cao W, Ramakrishnan R, Tyurin VA, Veglia F, Condamine T, Amoscato A, Mohammadyani D, Johnson JJ, Zhang LM, Klein-Seetharaman J, Celis E, Kagan VE, Gabrilovich DI. Oxidized lipids block antigen cross-presentation by dendritic cells in cancer. J. Immunol. 2014; 192:2920–2931. [PubMed: 24554775]

76. Kreso A, O'Brien CA, van Galen P, Gan OI, Notta F, Brown AMK, Ng K, Ma J, Wienholds E, Dunant C, Pollett A, Gallinger S, McPherson J, Mullighan CG, Shibata D, Dick JE. Variable clonal repopulation dynamics influence chemotherapy response in colorectal cancer. Science. 2013; 339:543–548. [PubMed: 23239622]

77. Marusyk A, Tabassum DP, Altrock PM, Almendro V, Michor F, Polyak K. Non-cell-autonomous driving of tumour growth supports sub-clonal heterogeneity. Nature. 2014; 514:54–58. [PubMed: 25079331]

78. Harding HP, Zhang Y, Bertolotti A, Zeng H, Ron D. Perk is essential for translational regulation and cell survival during the unfolded protein response. Mol. Cell. 2000; 5:897–904. [PubMed: 10882126]

79. Urano F, Wang X, Bertolotti A, Zhang Y, Chung P, Harding HP, Ron D. Coupling of stress in the ER to activation of JNK protein kinases by transmembrane protein kinase IRE1. Science. 2000; 287:664–666. [PubMed: 10650002]

80. Wu J, Rutkowski DT, Dubois M, Swathirajan J, Saunders T, Wang J, Song B, Yau GD-Y, Kaufman RJ. ATF6α optimizes long-term endoplasmic reticulum function to protect cells from chronic stress. Dev. Cell. 2007; 13:351–364. [PubMed: 17765679]

81. Hayashi MT, Cesare AJ, Fitzpatrick JAJ, Lazzerini-Denchi E, Karlseder J. A telomere-dependent DNA damage checkpoint induced by prolonged mitotic arrest. Nat. Struct. Mol. Biol. 2012; 19:387–394. [PubMed: 22407014]

82. Montague TG, Cruz JM, Gagnon JA, Church GM, Valen E. CHOPCHOP: A CRISPR/Cas9 and TALEN web tool for genome editing. Nucleic Acids Res. 2014; 42:W401–W407. [PubMed: 24861617]

83. Ran FA, Hsu PD, Wright J, Agarwala V, Scott DA, Zhang F. Genome engineering using the CRISPR-Cas9 system. Nat. Protoc. 2013; 8:2281–2308. [PubMed: 24157548]

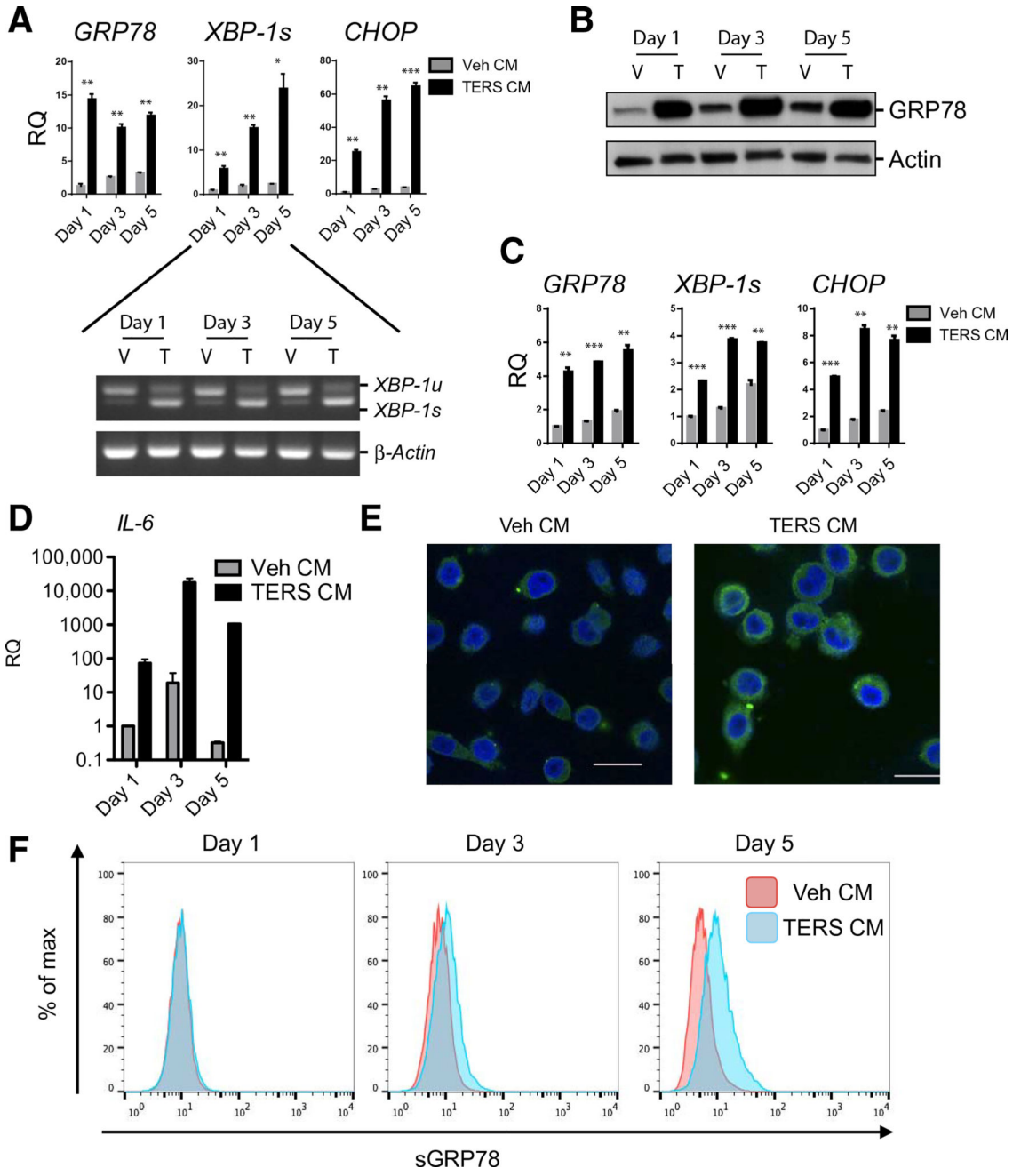

Fig. 1. Prostate cancer cells undergoing ER stress can transmit an ER stress response to recipient cells

(**A**) Expression of the indicated mRNA (by RT-qPCR) in PC3 cells cultured for 1, 3, or 5 days in Veh CM or TERS CM ($n = 2$ per condition). Gene expression was normalized to Veh CM day 1. RQ, relative quantification. Inset shows gel banding for unspliced (*XBP-1u*) and spliced (*XBP-1s*) *XBP-1*. (**B**) Western blot analysis for GRP78 abundance in whole-cell lysates from PC3 cells cultured as described in (A). V, Veh CM; T, TERS CM. (**C**) RT-qPCR in DU145 cells as described in (A) treated with PC3 generated Veh CM or TERS CM ($n = 2$ per condition). Gene expression was normalized to Veh CM day 1 condition to determine

relative quantification. (**D**) RT-qPCR analysis for *IL-6* expression in PC3 cells cultured with Veh CM or TERS CM as described in (A). Values are normalized to Veh CM day 1 ($n = 2$ per condition). (**E**) Confocal microscopy for GRP78 in Veh CM– or TERS CM–treated PC3 cells for 48 hours. Scale bars, 25 μm. (**F**) Flow cytometry analysis of surface abundance of GRP78 (sGRP78) in Veh CM– or TERS CM–cultured, unpermeabilized PC3 cells. Data are means ± SEM; $*P < 0.05$, $**P < 0.01$, $***P < 0.001$, paired two-tailed Student's *t* tests. Data in (C) to (E) are representative of two experiments; data in (A), (B), and (F) are from three independent experiments.

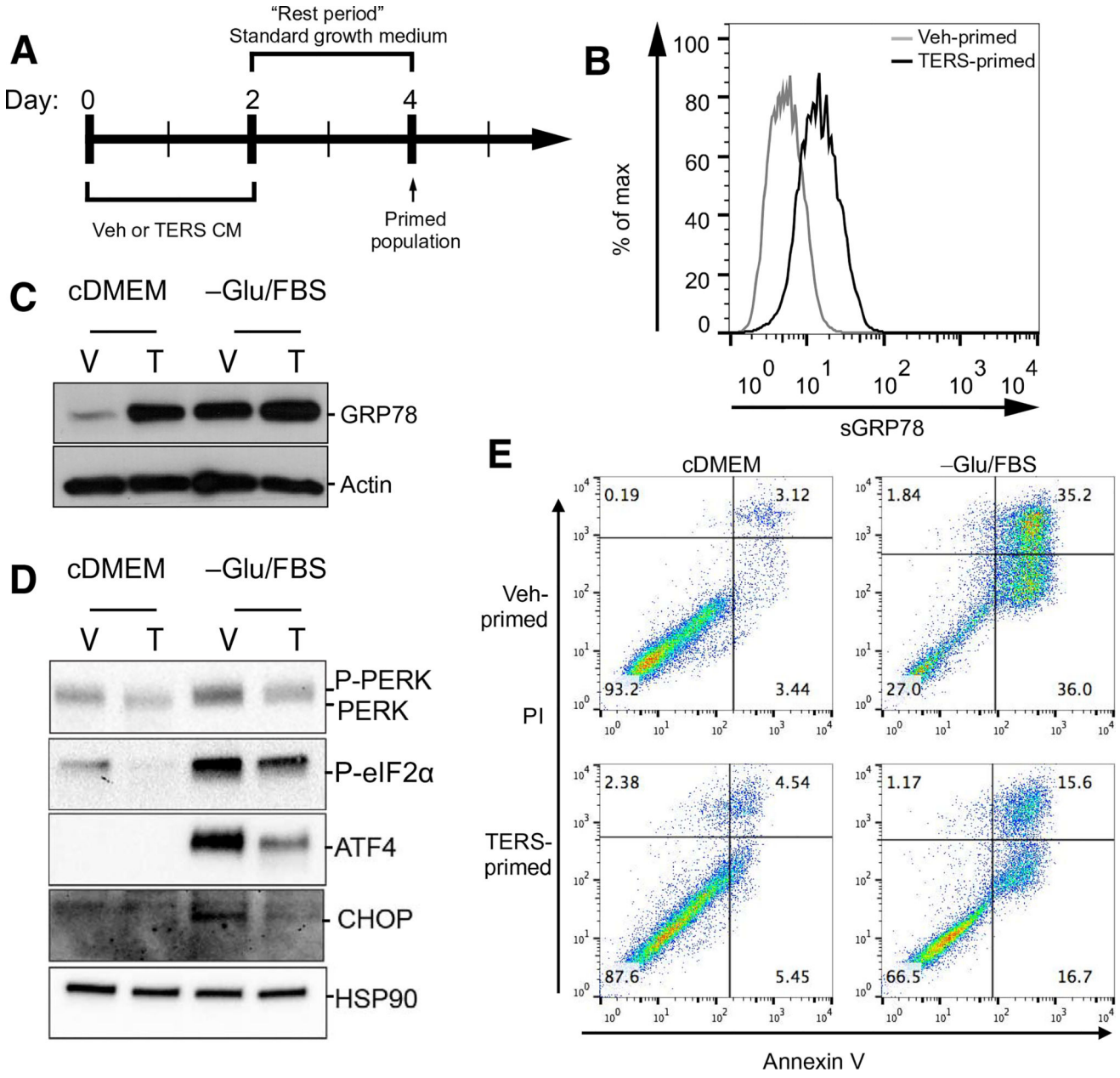

Fig. 2. TERS-primed cancer cells display a unique UPR and are protected against nutrient deprivation

(**A**) Treatment design of TERS priming: 2-day culture in Veh CM or TERS CM followed by 2-day rest period. Cells were then challenged and analyzed as indicated. (**B**) Flow cytometry analysis for surface abundance of GRP78 in vehicle- or TERS-primed PC3 cells grown in standard growth medium. (**C**) Western blot analysis of GRP78 in vehicle (V)– or TERS (T)–primed PC3 cells after 48-hour culture in standard growth medium (cDMEM) or in nutrient-deprived condition [-Glu/FBS (fetal bovine serum)]. (**D**) Western blot analysis of proteins of the PERK pathway in vehicle- or TERS-primed PC3 cells after 48-hour culture in cDMEM or in -Glu/FBS. (**E**) Apoptosis analysis by flow cytometry detection of annexin V in vehicle- or TERS-primed PC3 cells after 48-hour culture in cDMEM or in -Glu/FBS (each plot

represents at least 10,000 events per condition). Data in (D) are representative of two experiments; data in (B), (C), and (E) are from three or more independent experiments.

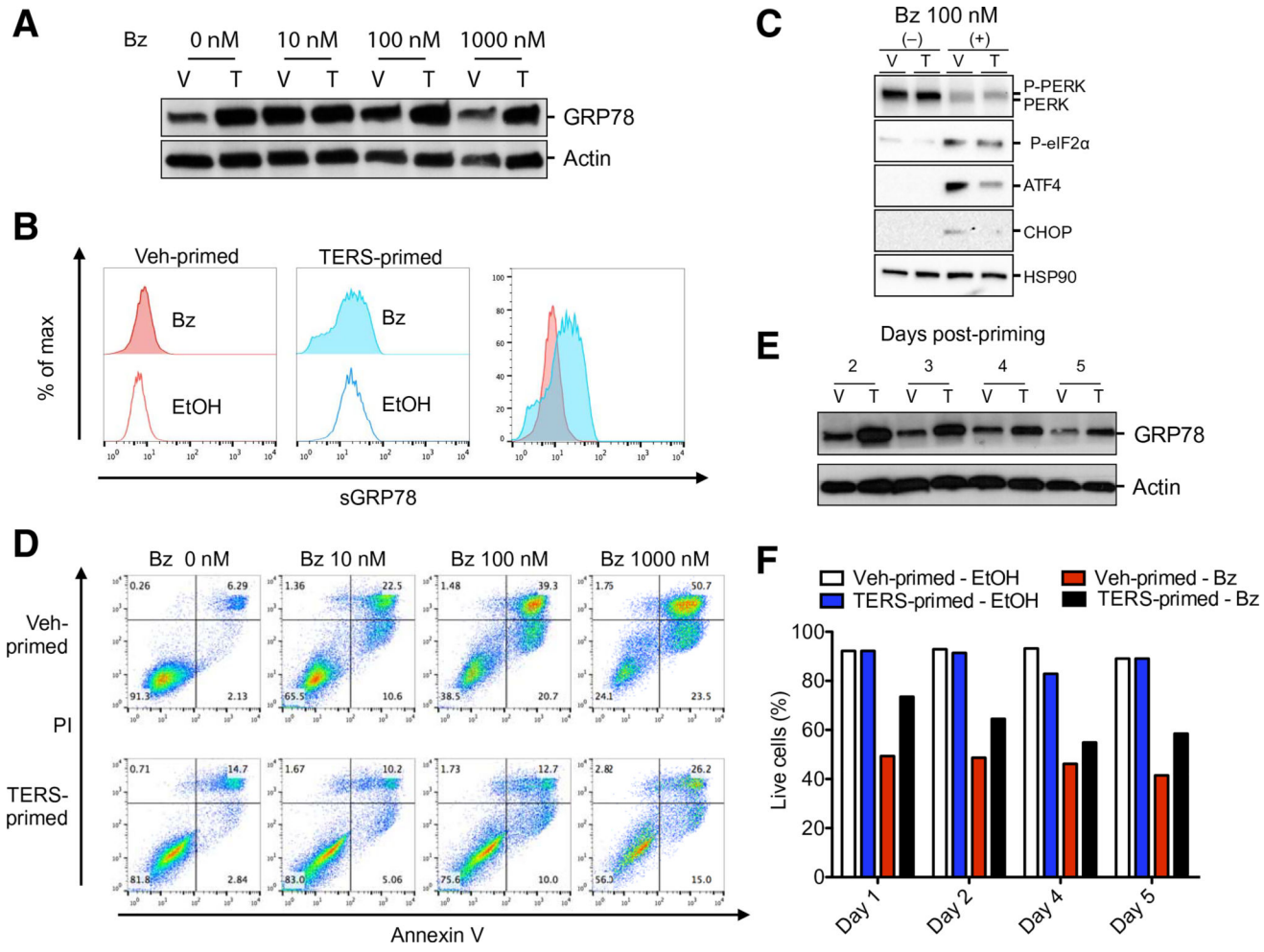

Fig. 3. Proteasome inhibition–mediated cytotoxicity is less effective in TERS-primed cells

(**A**) Western blot analysis of GRP78 in vehicle (V)– or TERS (T)–primed PC3 cells after 24-hour culture with various concentrations of bortezomib (Bz). (**B**) Flow cytometry analysis for the abundance of GRP78 (sGRP78) on the surface of vehicle- or TERS-primed PC3 cells 24 hours after EtOH control solution or bortezomib (100 nM) treatment. Data are shown individually and as an overlay for comparison. (**C**) Western blot analysis of PERK pathway proteins of vehicle- or TERS-primed PC3 cells 24 hours after addition of bortezomib. (**D**) Apoptosis analysis by annexin V/propidium iodide (PI) staining in vehicle- or TERS-primed PC3 cells 24 hours after addition of bortezomib (each plot represents at least 10,000 events per condition). (**E**) Western blot of GRP78 expression in vehicle- or TERS-primed PC3 cells cultured in cDMEM and harvested at the specified postpriming day. (**F**) Percent live cells determined by flow cytometry analysis of annexin V/PI apoptosis staining in vehicle- or TERS-primed PC3 cells treated with EtOH control solution or bortezomib (100 nM). Data in (A), (C), and (E) are representative of two experiments; data in (B) and (F) are from three experiments; data in (D) are from five independent experiments.

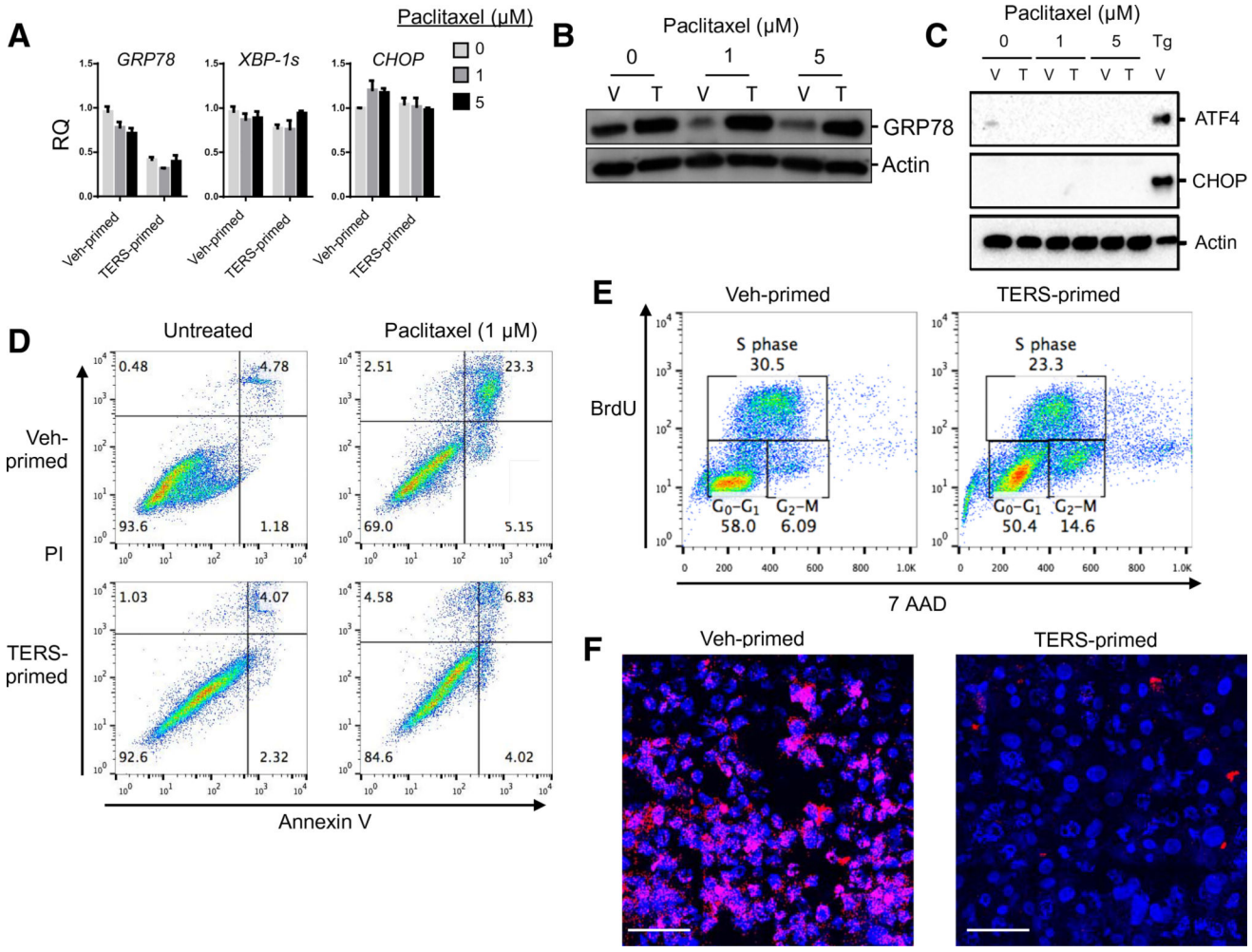

Fig. 4. TERS-primed cells are protected against genotoxic insults in the absence of ER stress

(**A**) Vehicle- or TERS-primed PC3 cells treated with increasing concentrations of paclitaxel and analyzed after 24 hours by RT-qPCR for relative gene expression of UPR genes. Samples were normalized to 0 μM vehicle–primed gene expression ($n = 2$ per condition). (**B**) Western blot analysis of GRP78 in PC3-primed cells treated with paclitaxel for 24 hours. (**C**) Western blot analysis of PERK signaling in PC3 vehicle- or TERS-primed cells treated with paclitaxel for 24 hours. PC3 cells treated with Tg (300 nM) serve as positive control. (**D**) Annexin V apoptosis assay of primed PC3 cells untreated or treated with paclitaxel for 48 hours (each plot represents at least 10,000 events per condition). (**E**) Cell cycle analysis as determined by BrdU incorporation in vehicle- or TERS-primed PC3 cells (each plot represents at least 10,000 events per condition). (**F**) DNA double-stranded breaks visualized through γ-H2AX staining (pink) and imaged by confocal microscopy in vehicle- or TERS-primed PC3 cells after 24-hour treatment with paclitaxel (1 μM). Scale bars, 100 μm. Data in (B), (C), and (F) are representative of two experiments; data in (A), (D), and (E) are from three or more independent experiments.

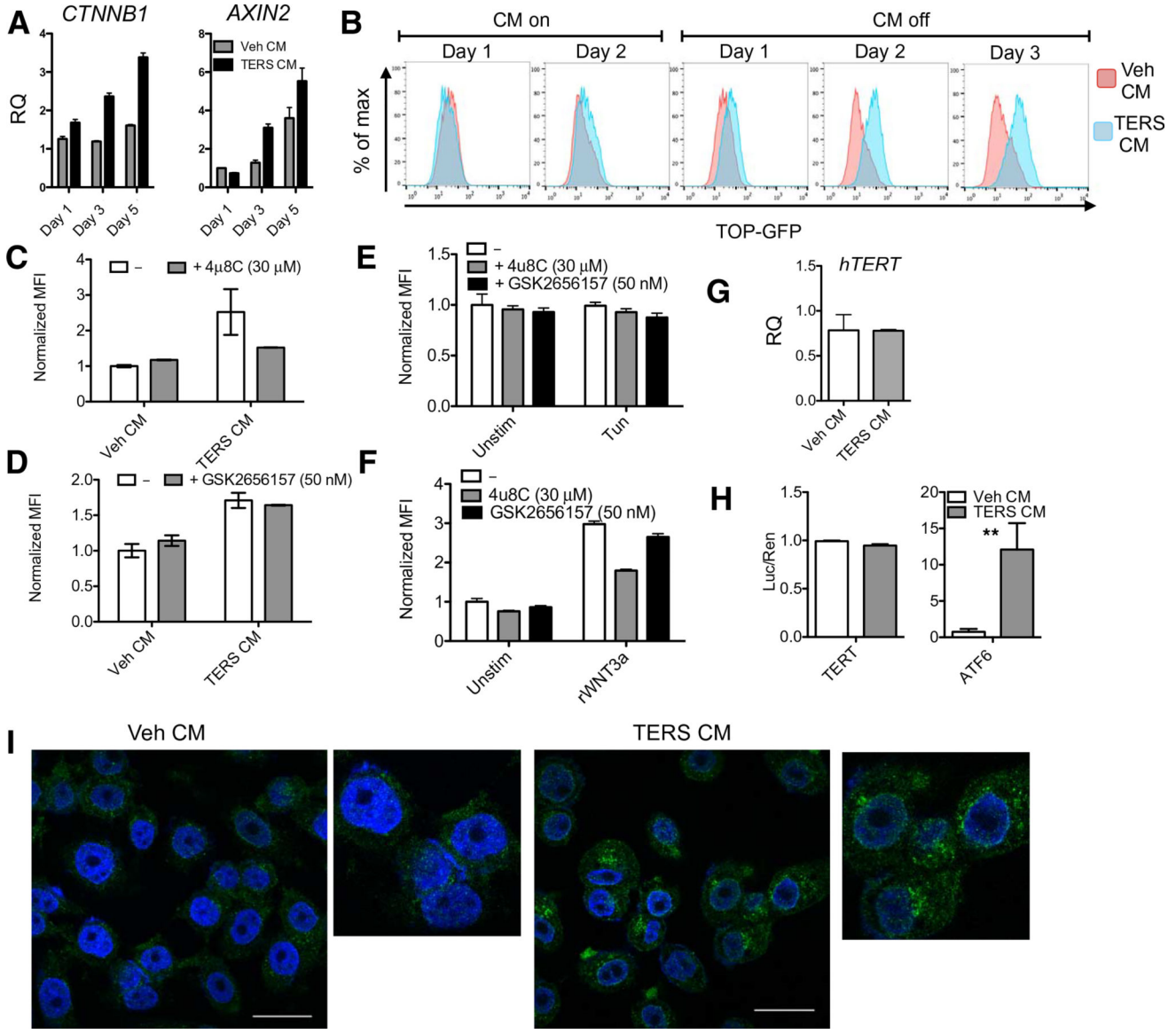

Fig. 5. TERS induces WNT signaling and cytoplasmic export of TERT

(**A**) RT-qPCR analysis of the transcriptional activation of *CTNNB1* and *AXIN2* of Veh CM– or TERS CM–treated PC3 cells throughout 5 days of culture with CM resupplementation every other day. Relative quantification of gene expression of samples is normalized to Veh CM day 1 condition ($n = 2$ per group). (**B**) TOP-GFP expression of PC3 cells during TERS priming, determined by flow cytometry (at least 10,000 events were analyzed per condition). PC3.TOP cells treated with Veh CM or TERS CM for 48 hours in the absence or presence of (**C**) the IRE1α inhibitor 4μ8C or (**D**) the PERK inhibitor GSK2656157 and measured for mean fluorescence intensity (MFI). MFI expression was then normalized to Veh CM uninhibited value ($n = 2$; at least 10,000 events were analyzed per condition). (**E**) Normalized MFI expression of PC3.TOP cells treated with tunicamycin (5 μg/ml) for 48 hours during IRE1α or PERK inhibition ($n = 2$; at least 10,000 events were analyzed per condition). (**F**) Normalized MFI expression of PC3.TOP stimulated for 48 hours with

recombinant WNT3a (rWNT3a) (20 ng/ml) during IRE1α or PERK inhibition ($n = 2$; at least 10,000 events were analyzed per condition). (**G**) *hTERT* RT-qPCR analysis of 48-hour Veh CM– or TERS CM–treated PC3 cells ($n = 3$ per condition). (**H**) Relative firefly TERT promoter-luciferase or ATF6 promoter-luciferase of dually transfected LNCaP cells. Cells were treated with LNCaP Veh CM or TERS CM for 48 hours and normalized for expression by *Renilla*-luciferase ($n = 3$ per condition). $^{**}P < 0.01$, Student's *t* test (paired two-tailed). (**I**) Immunofluorescence staining for TERT in PC3 cells treated for 48 hours. Scale bars, 25 μm. Error bars represent SEM. Data in (C), (D), and (H) are representative of two experiments; data in (A), (B), (F), (G), and (I) are from at least three independent experiments.

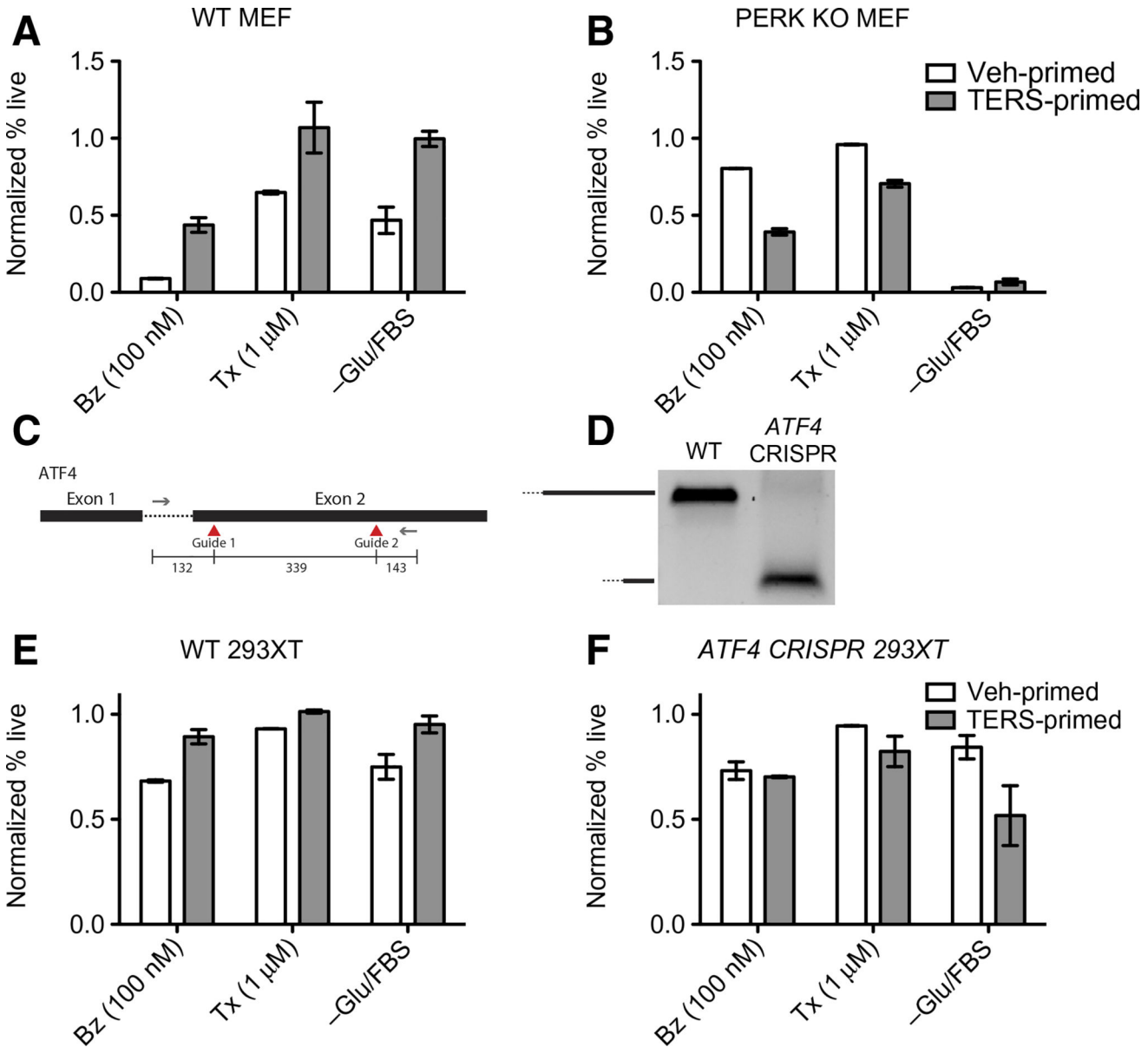

Fig. 6. PERK signaling is necessary for TERS-mediated cytoprotection

(**A** and **B**) Survival of (A) wild-type (WT) or (B) PERK KO MEFs primed by TC1 Veh CM or TERS CM and challenged for 48 hours as specified (Tx, paclitaxel). Survival determined by flow cytometry analysis via 7AAD exclusion. Percent (%) survival calculated by normalizing the percent live ($7AAD^-$) population of the unstimulated condition for each line ($n = 2$ per group; at least 10,000 events analyzed per condition). (**C**) CRISPR/Cas9 design of guide targets within the *ATF4* gene. (**D**) PCR detection of *ATF4* WT and *ATF4* CRISPR 293XT cells. WT 293XT (**E**) and ATF4 CRISPR 293XT (**F**) cells were primed with PC3 Veh CM or TERS CM, and survival was measured by 7AAD exclusion after 48 hours of treatment, as specified ($n = 2$ per condition; at least 10,000 events were analyzed per condition). Error bars represent SEM. Data in (A), (B), and (D) are representative of two experiments; data in (E) and (F) are from three independent experiments.

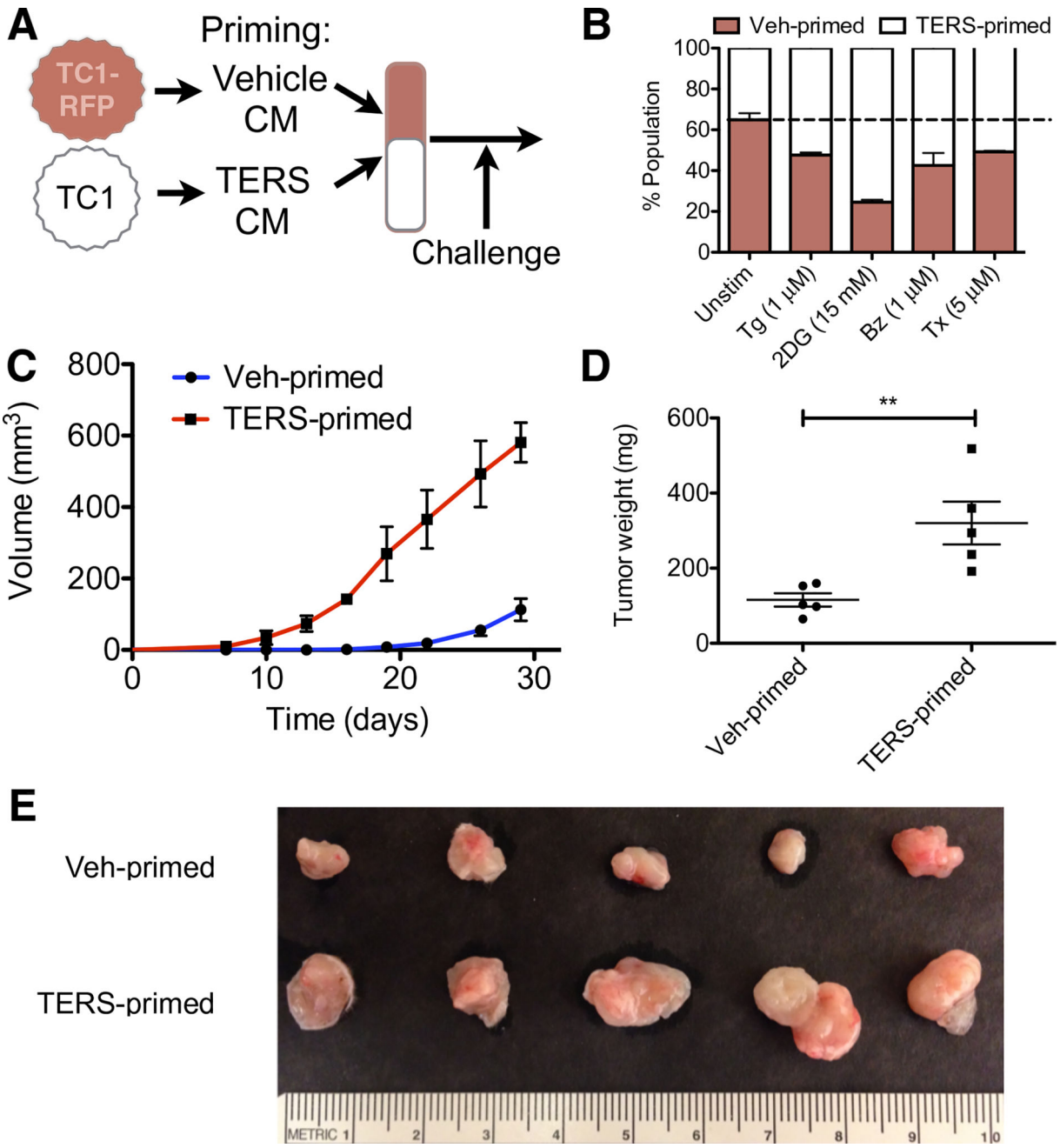

Fig. 7. TERS-primed murine prostate cancer cells have improved cellular fitness in vitro and in vivo

(**A**) Cartoon of coculture experimental design. Briefly, RFP-tagged TC1 cells (TC1-RFP) are primed with homologous Veh CM, whereas untagged TC1 cells are primed with TERS CM. After priming, cell populations are cocultured overnight and subsequently challenged. (**B**) Flow cytometry analysis to determine the percent RFP^+ (vehicle-primed) and RFP^- (TERS-primed) TC1 cells, 7AAD excluded, after 24-hour treatment with Tg, 2-deoxyglucose (2DG), bortezomib, or paclitaxel ($n = 2$ per coculture; at least 10,000 events were analyzed per condition). (**C**) Growth kinetics of vehicle- or TERS-primed TC1 cells subcutaneously

injected into immunocompetent C57BL/6 mice ($n = 5$ per group). (**D**) Weight of vehicle- or TERS-primed tumors after 30 days. (**E**) Gross visualization of excised tumors. $^{**}P < 0.01$, Student's t test (paired two-tailed). Error bars are SEM. Data are representative of two independent experiments.

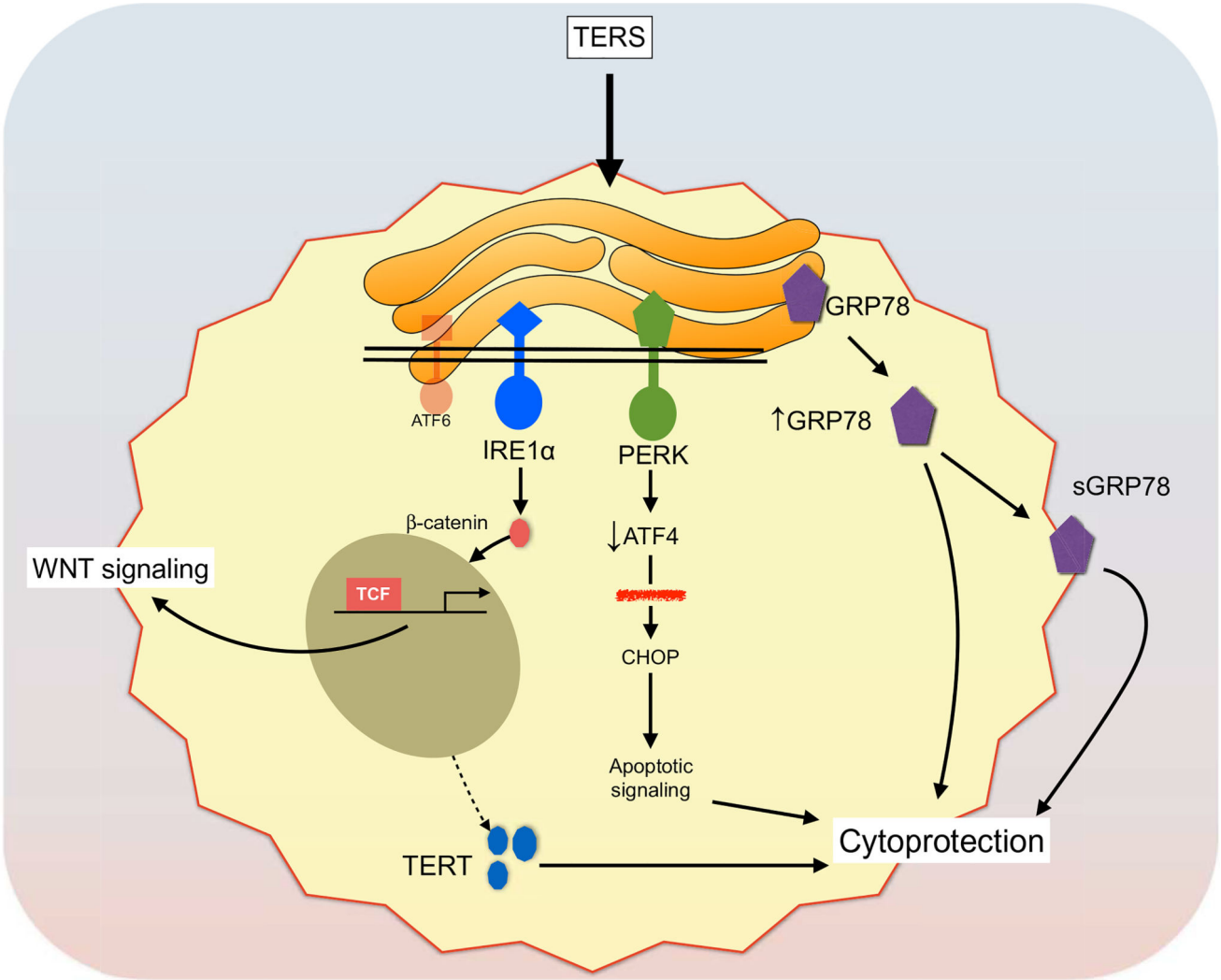

Fig. 8. Model of TERS-mediated signaling in cancer cells

We propose a model in which cancer cells exposed to TERS undergo an adaptive UPR that involves diverse signaling events. One effect is the activation of Wnt signaling. TERS drives Wnt signaling through the activation of the TCF. This effect appears to be IRE1α-dependent. The other relevant event is cytoprotection. In this case, TERS engages PERK but also leads to reduced ATF4 activation. Reduced levels of ATF4 are insufficient to drive full activation of apoptosis through the downstream CHOP target (red strikethrough). In this respect, ATF4 serves as a rheostat for cell survival. TERS also increases the amounts of GRP78, both intracellularly and at the cell surface. Finally, TERS induces the export of TERT to the cytoplasm. These effects, possibly in combination, promote cytoprotection and, ultimately, cell fitness to endogenous (nutrient) and exogenous (chemotherapeutic) stress.